Comptes Rendus
Géoscience — Sciences de la Planète
Published online: 12 January 2023
https://doi.org/10.5802/crgeos.179

Geo-hydrological Data & Models / *GDM - Géo-hydrologie, données et modèles*

Future climate or land use? Attribution of changes in surface runoff in a typical Sahelian landscape

Climat futur ou états de surface ? Contributions aux changements dans l'écoulement de surface en contexte Sahélien

Roland Yonaba [a,*], Lawani Adjadi Mounirou [a], Fowé Tazen [a], Mahamadou Koïta [a], Angelbert Chabi Biaou [a], Cheick Oumar Zouré [a], Pierre Queloz [b], Harouna Karambiri [a] and Hamma Yacouba [a]

[a] Laboratoire Eau, Hydro-Systèmes et Agriculture (LEHSA), Institut International d'Ingénierie de l'Eau et de l'Environnement (2iE), 01 BP 594 Ouagadougou 01, Burkina Faso

[b] Institute of Territorial Engineering (INSIT), School of Management and Engineering Vaud (HEIG-VD), Yverdon-les-Bains, Switzerland

E-mails: ousmane.yonaba@2ie-edu.org (R. Yonaba), adjadi.mounirou@2ie-edu.org (L. A. Mounirou), tazen.fowe@2ie-edu.org (F. Tazen), mahamadou.koita@2ie-edu.org (M. Koïta), angelbert.biaou@2ie-edu.org (A. C. Biaou), cheickoumar.zoure@gmail.com (C. O. Zouré), pierre.queloz@gmail.com (P. Queloz), harouna.karambiri@2ie-edu.org (H. Karambiri), hamma.yacouba@2ie-edu.org (H. Yacouba)

Abstract. In this study, the Soil and Water Assessment Tool (SWAT) model is used to assess changes in surface runoff between the baseline (1995–2014) and future (2031–2050) periods in the Tougou watershed (37 km^2) in Burkina Faso. The study uses a combination of land use maps (for current and future periods) and a bias-corrected ensemble of 9 CMIP6 climate models, under two warming scenarios. An increase in rainfall (13.7% to 18.8%) is projected, which is the major contributor to the increase in surface runoff (24.2% to 34.3%). The land use change narrative (i.e. conversion of bare areas to croplands) is expected to decrease in surface runoff, albeit minor in comparison to the effect of future climate change. Similar findings are observed for annual maximum surface runoff. This study sheds light on the need to consider simultaneously future climate and land use in framing water management policies.

Résumé. Dans cette étude, le modèle agro-éco-hydrologique SWAT est utilisé pour évaluer les changements dans l'écoulement de surface entre la période de référence 1995–2014 et future 2031–2050 sur le bassin versant de Tougou (37 km^2) au Burkina Faso. Cette étude utilise une combinaison de cartes d'états de surface (pour la période actuelle et future) et un ensemble corrigé de 9 modèles climatiques issus des simulations CMIP6, sous deux scénarios de réchauffement. Une augmentation des

* Corresponding author.

précipitations (de 13,7 % à 18,8 %) est prévue, ce qui est le principal facteur contribuant à l'augmentation des écoulements de surface (24,2 % à 34,3 %). Les changements projetés sur les états de surface (principalement la conversion des surfaces dégradées en sols cultivés) devrait entraîner une diminution des écoulements de surface, toutefois dans des proportions plus faibles en comparaison des effets du climat futur. Des résultats similaires sont observés pour lécoulement de surface maximal annuel. Cette étude met en lumière la nécessité de prendre en compte simultanément le climat futur et les changements sur les états de surface dans l'élaboration des politiques futures de gestion de l'eau.

Keywords. Climate change, Hydrological modelling, Land use/land cover change, Sahel, Surface runoff, SWAT, Tougou watershed.

Mots-clés. Changement climatique, Modélisation hydrologique, Changement d'affectation des terres et de la couverture végétale, Sahel, Ecoulement de surface, SWAT, Bassin versant de Tougou.

Published online: 12 January 2023

1. Introduction

In the hydrological cycle, the factors driving catchment-scale processes are mainly climate and land use [de Marsily, 2007]. Here, "*land use*" both includes land cover, land use and land management [Yin et al., 2017]. Climate change and variability are primarily driven by large scale conditions and result in global and regional substantial changes [Bhagat et al., 2022, Connors et al., 2022, IPCC, 2022]. Locally mitigating the harming impacts of climate change on the water cycle could be fostered by informed land use and water management at the community level [Zipper et al., 2018].

The issue is more acute to the West African Sahel, which is known to be an ecoclimatic context strongly affected by intense droughts, severe rainfall deficits and increased rainfall variability driven by abrupt climate oscillations [Biasutti, 2019]. The region also features the highest populations exerting strong pressure on natural resources (land clearing for cropping, ecosystem services). Besides, the capacity of populations living in these regions to adapt to climate change and variability impacts remains low [Serdeczny et al., 2017]. In such drought-prone contexts, improving local resilience through integrated water management should both consider land use decisions, water use and allocation [Belemtougri et al., 2021, Fovet et al., 2021, Kafando et al., 2021, Zipper et al., 2018]. This, in turn, requires, at the core, a deeper understanding of the individual and combined contributions of climate and land use changes on the hydrological cycle, which is generally not well assessed, especially for such West African watersheds [Aich et al., 2015, Yira et al., 2017, Yonaba, 2020, Gbohoui et al., 2021, 2022].

The complexity of processes in the water cycle in Sahelian watersheds remains a major challenge to hydrologists to date, for various reasons: first, rainfall conditions in this context are specifically defined by high intensities rainfall of short durations [Biasutti, 2019], which quickly onsets a highly nonlinear Hortonian surface runoff response [Mounirou et al., 2020]. Second, surface runoff generation mechanisms are typically dependent on both antecedent rainfall but also soil surface conditions, the latter being prone to surface crusting and sealing; which, in turn, affects other key processes such as infiltration, and evaporation [Valentin, 2018, Zouré et al., 2019]. Third, long-term and spatially complete sets of rainfall-runoff observations are scarce and rarely gap-free, since monitoring networks are lacking [Mahé and Paturel, 2009]. These conditions severely hamper hydrological modelling applications in these contexts, which are nevertheless the preferred approach to assess the combined and individual contributions of climate and land use dynamics on the water cycle [Yin et al., 2017].

To the best of our knowledge, few modelling studies in the Sahel have been dedicated to this exercise still [Aich et al., 2015, Akoko et al., 2021, Angelina et al., 2015, Dembélé et al., 2022, Gal et al., 2017, Grippa et al., 2017, Karambiri et al., 2011, Séguis et al., 2004]. Among the reasons often put forward, some authors mention the difficulty in representing accurately Sahelian hydrological processes in most of the available models [Cornelissen et al., 2013, Karambiri et al., 2003], or the data scarcity [Mahé and Paturel, 2009]. Another difficulty in achieving accuracy in simulating the water balance in hydrological models resides in a full acquaintance of land use/land cover changes (LULCC) during long-term runs in modelling experiments. Usually, a single and static LULC map of the landscape at a given time point is used, which might lead to failure in picturing the spatial and temporal patterns of evolution of hydrological

processes [Wagner et al., 2016, Yonaba et al., 2021a]. Some hydrological models, such as the Soil and Water Assessment Tool [Arnold et al., 1998] provide mechanisms to integrate a dynamical update of LULC conditions during simulations, through a dedicated land use update (LUP) module, which reportedly helped in achieving significant higher model performance [Aghsaei et al., 2020, Yonaba et al., 2021a].

The question of which of the two factors between climate and land use changes is mainly responsible for the alteration of hydrological processes is yet to be answered in the case of Sahelian watersheds. The most often occurring landscape trajectory in this region is the loss of natural vegetation, which has been primarily associated with the increase in surface runoff [Amogu et al., 2015, Gal et al., 2017, Yonaba, 2020]. Yet, some studies highlight that the attribution of the observed changes in surface runoff remains unclear, probably without a single definitive answer across all contexts [Aich et al., 2015, Descroix et al., 2018]. Regarding climate change, most future climate projections converge for warming in average temperatures and an increase in potential evapotranspiration over the Sahel [Diedhiou et al., 2018], whereas for rainfall, forecasts remain mixed [Dosio et al., 2020]. Such perspectives are leaving large uncertainties about the overall impact of climate or LULC change on the hydrological cycle [Stanzel et al., 2018, Sylla et al., 2018, Todzo et al., 2020].

To meet this challenge, in this study, we introduce a methodological framework to assess the combined and relative contribution of future climate and LULC changes on the hydrological cycle, with a focus on surface runoff, in a typical Sahelian landscape under semi-arid climate. The Tougou watershed (37 km^2), located in northern Burkina Faso, has been an observatory for the study of interrelations between climate, environment and population dynamics for more than 5 decades [Yonaba, 2020] and is selected as a support for this research. In a previous study, LULC maps of the Tougou watershed have been produced using remote sensing for the years 1999, 2009 and 2017; the landscape evolution has also been projected to 2030, 2040 and 2050, through land change modelling, under the hypothesis of business as usual trends [Yonaba et al., 2021b]. Also, the SWAT model has been calibrated based on rainfall-runoff observations between 2000 and 2017, using dynamics LULCs maps available for this period [Yonaba et al., 2021a]. Building upon these results, the aim of this study is twofold: (i) to forecast the projected changes in the hydrological balance using future climate and land use; (ii) to quantify the combined and individual contribution of climate and land use to average annual and daily extreme surface runoff.

2. Materials and methods

2.1. *Study area*

2.1.1. *Location and physical setting of Tougou watershed*

The study is carried out in the Tougou watershed (13.65° N; 2.26° E), which lies in north-eastern Burkina Faso, in the upper Nakanbe River Basin, within the Yatenga province. The location of the watershed, covering an area of 37 km^2, is shown in Figure 1a. The climate on the watershed is semi-arid, with a single rainy season from July to October. The major soils types (Figure 1b) are slightly evolved soils (25% of the area), crude mineral soils (35% of the area, prone to physical degradation into glacis) and hydromorphic soils (40% of the area) [IGB, 2002]. Elevation on the watershed varies between 318 to 338 meters, with slopes between 0–17% (Figure 1c).

According to the meteorological records provided by the National Meteorology Agency (ANAM-BF), over the reference period 1995–2014, the average annual rainfall is 700 mm. Daily temperatures range from 12 to 45 °C. The vegetation cover is sparse on the watershed and mostly made of savannah, shrubs, steppes and agrarian parklands. The drainage network consists of a dendritic network of ephemeral streams, collecting overland runoff to a main and intermittent river, long of 8 km [Mounirou, 2012, Yonaba, 2020].

2.1.2. *LULC evolution in Tougou watershed*

Land use maps of the Tougou watershed for the years 1999, 2009 and 2017 (Figure 2a–c) have been previously produced in Yonaba et al. [2021b] through the analysis of Landsat satellite images. A land change model built around a Multilayer Perceptron neural network has been used, in conjunction with population growth trends, to further forecast the land use maps of the watershed in 2030, 2040 and 2050 (Figure 2d–f), under a business-as-usual scenario [Yonaba et al., 2021b]. The land use categories

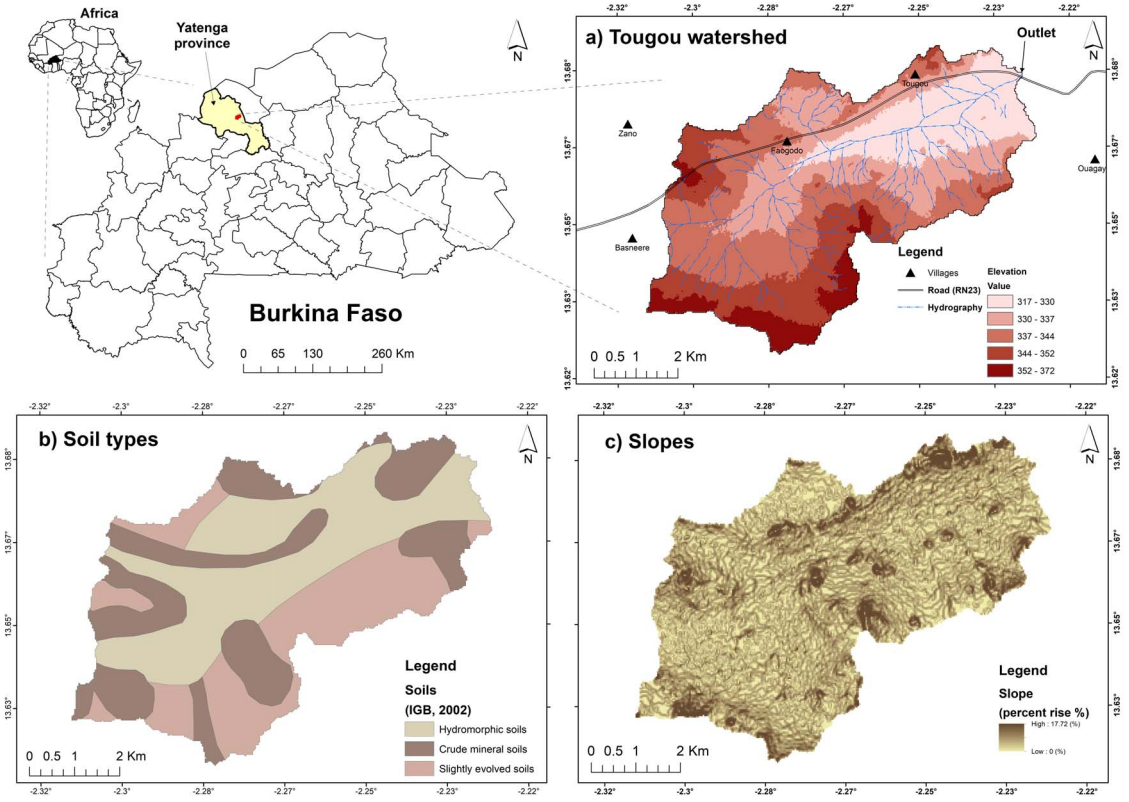

Figure 1. Location of the Tougou watershed (northern Burkina Faso). (a) Elevation and hydrography. (b) Soil types [IGB, 2002]. (c) Slope map, derived from elevation map.

considered in these maps are natural vegetation, bare lands and croplands. Natural vegetation areas are under permanent vegetation all the year-round, covered with herbaceous plants, shrub or trees; they are mostly found along the main river channel in the watershed. Bare lands exhibit a typically very low vegetation cover (less than 5%), made of residual clumps and herbaceous, with crusts and sealing developing at the surface, therefore limiting infiltration. Croplands are growing cereals (millet, sorghum) in the wet season (early June to mid-October), during which traditional farming practices are carried out on these soils to sustain crop production [Zouré et al., 2019, Yonaba et al., 2021b]. In the watershed, populations are relying of traditional wells (of 15–30 m depth) for water consumption; however, the amounts of such withdrawals are negligible [Rusagara et al., 2022] and were therefore not considered in this study.

In total, from 1999 to 2050, croplands are projected to increase from 48.6% to 86.6%, bare lands to decrease from 44.8% to 10.7% whereas natural vegetation is expected to decrease from 6.6% to 2.7%. The large increase in croplands is mostly driven by the population growth trends. Conversely, the land use type targeted for conversion to croplands is bare land, thanks to the wide array of farming techniques and soil conservation measures introduced in the region since the 1990s [Lèye et al., 2021, Nyamekye et al., 2018, Zouré et al., 2019].

2.2. *Overview of the methodology used in this study*

The general methodology adopted in this study is presented in Figure 3. The major steps consisted in selecting CMIP6 Global Circulation Models (GCM), then carrying out a bias correction of these models using observations during the baseline period 1995–2014. The SWAT model is then used to simulate hydrological processes in the baseline period (using

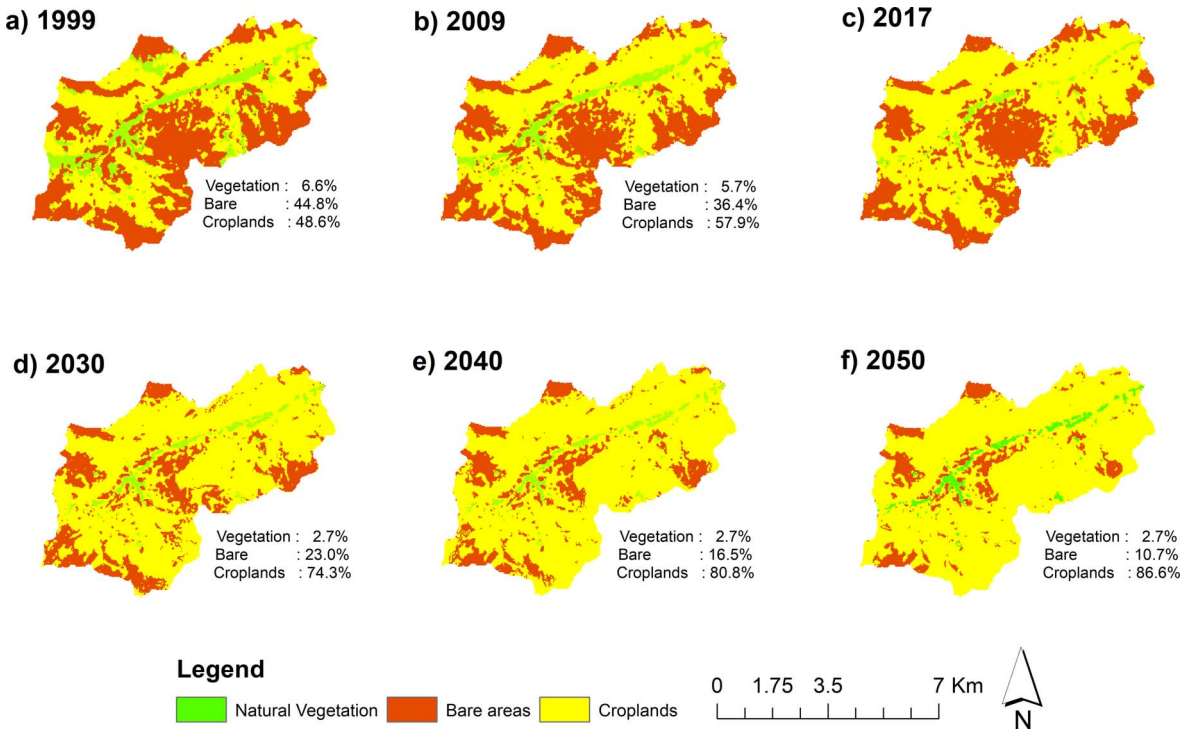

Figure 2. Land use maps of Tougou watershed for the period 1999–2050. Land use maps in 1999, 2009 and 2017 were produced through remote sensing images analysis. Land use maps in 2030, 2040 and 2050 were produced through land change modelling. Further details are given in Yonaba et al. [2021b].

LULC maps in 1999, 2009 and 2017), and the future period (using future LULC maps in 2030, 2040 and 2050). The comparison of changes in surface runoff under baseline and future conditions is used to assess the relative contributions of climate and land use changes.

2.3. *Estimation of daily potential evapotranspiration (PET)*

The observed climate variables available for the baseline period (1995–2014) are rainfall (*pr*), average daily temperature (*tas*), minimum daily temperature (*tasmin*), maximum daily temperature (*tasmax*), both provided by the National Meteorology Agency (ANAM-BF), at the daily timestep. Therefore, the use of the reference FAO-56 Penman–Monteith (PM) method is not applicable. To estimate daily PET, the Hargreaves–Samani (HS) equation [Hargreaves and Samani, 1985] is therefore selected as an alternative for its parsimonious estimation of PET solely relying on temperature data, which is available for the considered baseline period. The HS equation is given as in Equation (1) [Raziei and Pereira, 2013]:

$$\mathrm{PET} = 0.0135 k_{rs} \frac{R_a}{\lambda} (T_x - T_n)^n (T_m + b) \qquad (1)$$

where R_a is the extraterrestrial radiation (MJ·m^{-2}·d^{-1}), λ the latent heat of vaporization (2.45 MJ·kg^{-1}), T_x, T_n and T_m are respectively the daily maximum, minimum and average temperatures (°C). In Equation (1), k_{rs}, n and b are coefficients, originally defined as 0.17, 0.5 and 17.8 respectively [Raziei and Pereira, 2013].

Previous studies reported the reliability of HS equation for PET estimation in Burkina Faso, yet highlighted significant biases often occurring in daily estimates, which can be further reduced by calibrating the empirical coefficients in the formula against reference data [Ibrahim, 2002, Ndiaye et al., 2017, Zouré, 2019, Yonaba, 2020]. In this study, these coefficients were calibrated for each month in

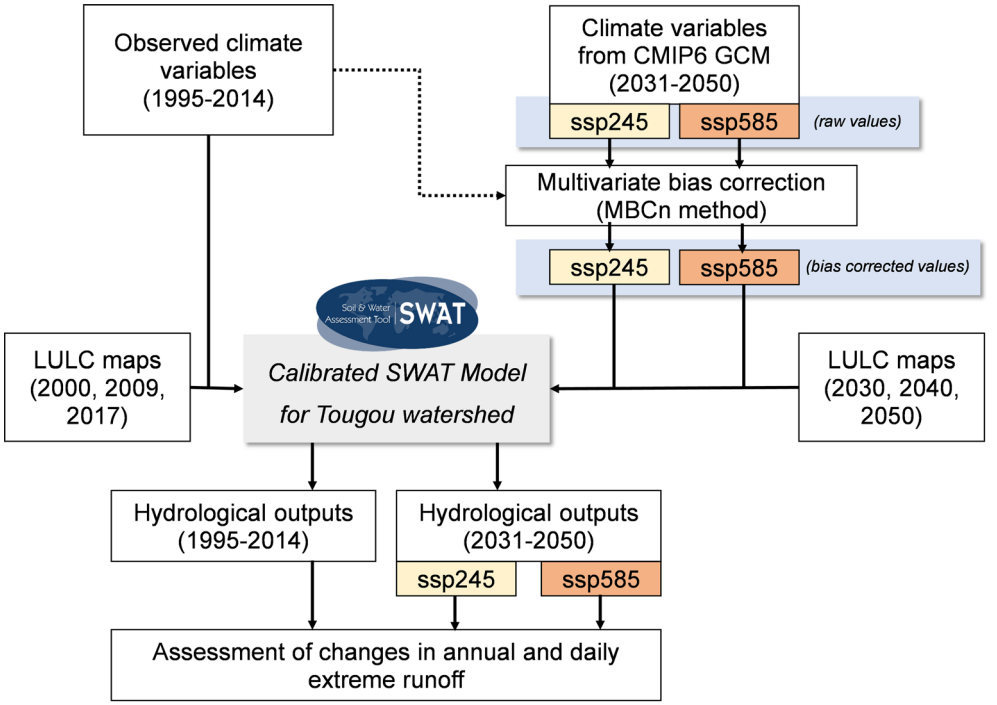

Figure 3. Flowchart of the study methodology.

the year, using PET data calculated from Penman–Monteith (PM) reference model over the previous period 1985–1994 (for which complete climate data were available). The calibration procedure is carried out using an adaptive non-linear least squares algorithm. The improvement of the calibration step is evaluated through graphical methods (including scatterplots and box-plots) and also statistical evaluation (coefficient of determination—R^2, Mann–Whitney U-test for the mean at $\alpha = 5\%$ significance level, root mean square error—RMSE, and percent bias—PBIAS) Some of these metrics are calculated as in Equation (2):

$$\begin{cases} R^2 = 1 - \dfrac{\sum_{i=1}^{n}(x_i^{\mathrm{PM}} - x_i^{\mathrm{HS}})^2}{\sum_{i=1}^{n}(x_i^{\mathrm{PM}} - \overline{x_i^{\mathrm{PM}}})^2} \\ \mathrm{RMSE} = \sqrt{\dfrac{1}{n}\sum_{i=1}^{n}(x_i^{\mathrm{HS}} - x_i^{\mathrm{PM}})^2} \\ \mathrm{PBIAS}\,(\%) = 100 \times \dfrac{1}{n}\sum_{i=1}^{n}\left(\dfrac{x_i^{\mathrm{PM}} - x_i^{\mathrm{HS}}}{x_i^{\mathrm{PM}}}\right) \end{cases} \quad (2)$$

where x_i^{HS} and x_i^{PM} are daily PET calculated with HS and PM equations respectively, $\overline{x_i^{\mathrm{PM}}}$ is the average over x_i^{PM} values and n the length of the dataset.

2.4. *Processing future climate projections*

2.4.1. *Selection of GCM models*

In this study, CMIP6 climate projections [Eyring et al., 2016] are used to project the future hydrological response. The data were retrieved from Copernicus Climate Data Store (CDS, https://cds.climate.copernicus.eu/cdsapp#!/dataset/projections-cmip6) for the baseline period 1995–2014 and the future period 2031–2050. Two Shared Socio-Economic Pathways (SSP) are considered: SSP2-4.5, a modest mitigation case scenario, standing as a most-plausible near future outcome (~2.5 °C global warming by 2100, relative to pre-industrial levels); and SSP5-8.5, a worst-case scenario defined by business-as-usual fossil-fuel intensive use, stringent of climate mitigation (~5 °C warming by 2100). The choice of these scenarios is also influenced by the fact that they remain comparable to the previous Representative Concentration Pathways (RCP) 4.5 and 8.5 scenarios, issued from CMIP5 and broadly used in past studies [Ayugi et al., 2022]. It is noteworthy to outline that as compared to the land use narratives in the Shared Socio-Economic Pathways

Table 1. List of CMIP6 models used in this study

In this study	Abbreviation	Model name
M1	ACCESS-CM2	Australian Community Climate and Earth System Simulator Model Version 2
M2	CNRM-CM6-1	Centre National de Recherches Meteorologiques Model Version 6.1
M3	CNRM-ESM2-1	Centre National de Recherches Meteorologiques—Earth System Model Version 2.1
M4	INM-CM4-8	Institute for Numerical Mathematics (INM) Model Version 4.8
M5	INM-CM5-0	Institute for Numerical Mathematics (INM) Model Version 5
M6	MIROC6	Model for Interdisciplinary Research on Climate Version 6
M7	MIROC-ES2L	Model for Interdisciplinary Research on Climate—Earth System Model
M8	MPI-ESM1-2-LR	Max-Planck-Institut für Meteorologie—Earth System Model
M9	MRI-ESM2-0	Meteorological Research Institute Earth System Model Version 2.0

(SSPs) scenarios, the LULC futures in Tougou watershed used in this study are more in line with the "*middle of the road*" SSP2-4.5 scenario [Popp et al., 2017].

The initial set of models available within the CDS archive was filtered to retain only models providing complete daily data for rainfall, temperature (minimum, maximum and average) and for both SSP2-4.5 and SSP5-8.5 pathways. An ensemble of 9 climate models, listed in Table 1, is finally considered for this study. These models all have a horizontal resolution of 250 km and are issued from the same ensemble member (*r1i1p1f1*).

2.4.2. *Multivariate bias correction of future climate data*

GCM outputs generally feature systematic biases over the historical baseline, which needs to be removed before their use in impact studies. To address this issue, the application of bias correction techniques is recommended [Dieng et al., 2022]. In this study, a multivariate trend preserving bias correction method, termed as *MBCn* [Cannon, 2018] is used. The general steps of application of this method are as follows: (1) the data for each variable of interest are pooled by individual months in the baseline (1995–2014) and the future (2031–2050) periods; (2) for each climate model and for each time series (one for each month), model-projected quantiles are detrended, then adjusted through quantile mapping constructed from a sampling of the baseline observations. In this study, a sampling of 50% of the observations is used to construct the optimal targeted quantile distributions; then, the initial trends are reintroduced. These steps form the so-called *Quantile Delta Mapping* (QDM) bias-correction, which is further detailed in Cannon et al. [2015]. The *MBCn* algorithm further comes as a multivariate generalization of the QDM method for simultaneous bias-correction of multiple variables, to preserve joint dependence [Cannon, 2018].

The bias-corrected variables in this study are daily rainfall and temperatures (average, minimum and maximum). Future daily PET is further calculated with the calibrated HS equation (presented in Section 2.3). This strategy is adopted here since correcting biases in dependent variables (here, temperature) has the potential of significantly reduce biases in PET forecasts [Yang et al., 2021].

2.5. *Hydrological simulation*

The SWAT model is used in this study for the simulation of hydrological processes in the Tougou watershed. SWAT is a physically-based and semi-distributed hydrological model, which simulates hydrological processes at the scale of Hydrological Response Units (HRUs) [Arnold et al., 1998]. The water balance equation as represented by the SWAT model is given by Equation (3):

$$\begin{aligned} \mathrm{SW}_t \;=\; \mathrm{SW}_0 + \sum_{i=1}^{t} (P_{\mathrm{day}} - Q_{sf,\mathrm{day}} \\ - \mathrm{ET}_{\mathrm{day}} - w_{\mathrm{seep,day}} - Q_{gw,\mathrm{day}}) \end{aligned} \tag{3}$$

where SW_t and SW_0 are the final and initial soil water (respectively), t is the elapsed time (in days), P_{day} is the daily rainfall, $Q_{sf,\mathrm{day}}$ is the daily surface runoff,

ET_{day} is the daily actual evapotranspiration, $w_{seep,day}$ is the daily seepage from the soil profile to the vadose zone and $Q_{gw,day}$ is the daily return flow from the aquifer. The surface runoff in the SWAT model is calculated using the empirical Soil Conservation Service (SCS) Curve Number (CN) method, given as in Equation (4) [Neitsch et al., 2011]:

$$Q_{sf,day} = \frac{(P_{day} - I_a)^2}{P_{day} - I_a + S}; \quad S = 25.4\left(\frac{1000}{CN} - 10\right) \tag{4}$$

where I_a is the sum of initial abstractions (including soil surface storage, interception and infiltration prior to the onset of runoff) and S is a retention parameter, which is controlled by spatial variations in soils, land use, management and slope. The CN parameter is therefore tabulated for all these conditions [Neitsch et al., 2011].

The SWAT model for the Tougou watershed was built using the elevation data from ASTER GDEM Digital Elevation Model, the soil map from the National Geographic Institute in Burkina Faso [IGB, 2002] and the available land use maps from Yonaba et al. [2021b]. The Land use Update (LUP) module within the SWAT model [Moriasi et al., 2019, Pai and Saraswat, 2011] is used to activate dynamic changes in land use during the simulations. The simulation during the baseline period used land use maps in 1999, 2009 and 2017, whereas the simulation during the future period used projected land use maps in 2030, 2040 and 2050.

The SWAT model has been previously calibrated for the Tougou watershed (over the period 2004–2018) with satisfactory performance (*Kling-Gupta efficiency*: KGE = 0.95/0.94; *percent bias*: PBIAS = −2.30%/2.90% for calibration/validation periods). The Table 2 is adapted from Yonaba et al. [2021a] and shows the calibrated values (and uncertainty range) for the model parameters, which were used in this study for hydrological simulation. Among these parameters, CN2 (SCS Curve Number), SOL_AWC (soil water content), ESCO (soil evaporation compensation factor), OV_N (Manning's n roughness for overland flow), SOL_K (saturated hydraulic conductivity) are the ones which are affected straight by land use [Amogu et al., 2015, Gal et al., 2017, Descroix et al., 2018, Yonaba et al., 2021a].

2.6. *Extreme value analysis*

Extreme values (EV) often constitute the rationale for designing hydraulic structures for flood control, or devise mitigation strategies for water management at the community level. Such extremes are likely to be affected by land use or climate change [Hounkpè et al., 2019, Tazen et al., 2019]. In this study, different EV distributions (including Gumbel, GEV, Gamma, Weibull) were fitted over the daily annual maximum rainfall and annual maximum surface runoff values distributions over the baseline period 1995–2014. The quality of the fit was evaluated using the Kolmogorov–Smirnov test (at $\alpha = 5\%$ significance level). The three-parameter Weibull distribution (W3) was finally selected as the optimally fitting EV distribution (p-value = 0.992 and 0.945 for rainfall and surface runoff extremes respectively) and is therefore used in this study, similarly as in Sawadogo and Barro [2022] in Burkina Faso, or in Li et al. [2015] and Olivera and Heard [2019]. The probability density function (PDF) and the quantile (inverse cumulative distribution function) of this distribution are given in Equation (5):

$$\begin{cases} f_{(x)} = \dfrac{\beta}{\gamma}\left(\dfrac{x-\mu}{\gamma}\right)^{\beta-1} \mathrm{e}^{-(\frac{x-\mu}{\gamma})^{\beta}} \\ Q_{(p)} = \gamma(-\ln(1-p))^{1/\beta} + \mu \end{cases} \tag{5}$$

where $x > \mu$ is a given quantile, β, γ and μ are the shape, scale and location parameters of the Weibull distribution (respectively), $p = 1 - (1/T)$ is the non-exceedance probability associated with the return level T in years. The quality of the W3 fit was assessed through the non-parametric Kolmogorov–Smirnov test (at $\alpha = 5\%$ significance level).

The fitted W3 distributions are used to derive extreme daily rainfall and surface runoff for 2, 5, 10, 15, 20, 25 and 30-years return periods. These values are further used to assess the various contributions of climate and land use change on surface runoff extremes.

2.7. *Evolution of ecohydrological signatures*

To assess the change in ecohydrological signatures of the Tougou watershed between the baseline and the future periods, the water-energy budget of Tomer and Schilling [2009] is used in this study. This framework states that as the climate change signal affects

Table 2. Calibrated SWAT model parameters in Tougou watershed

Parameter	Description (Unit)	Calibration method	Initial range	Fitted values (Uncertainty range)
CN2	SCS Curve number (-)	r	−0.3–0.3	−0.0787 (−0.249; 0.057)
EPCO	Plant uptake compensation factor (-)	v	0–1	0.2036 (0.091; 0.402)
SOL_K	Saturated hydraulic conductivity ($mm{\cdot}h^{-1}$)	r	−0.3–0.3	−0.0232 (−0.157; 0.272)
GW_DELAY	Groundwater delay time (days)	v	0–500	52.584 (25.203; 53.799)
RCHRG_DP	Deep aquifer percolation fraction (-)	v	0–1	0.3566 (0.078; 0.239)
GW_REVAP	Groundwater "revap" coefficient (-)	v	0.02–0.2	0.0948 (0.065; 0.156)
OV_N	Overland flow Manning roughness ($s{\cdot}m^{-1/3}$)	r	−0.3–0.3	−0.3038 (−0.595; 0.152)
CH_K2	Hydraulic conductivity in channels ($mm{\cdot}h^{-1}$)	v	0–300	50.173 (23.66; 114.30)
SOL_AWC	Available soil water content (mm)	r	0–0.5	0.3707 (0.326; 0.405)
REVAPMN	Threshold depth of water for "revap" (mm)	v	0–500	344.08 (247.69; 416.06)
CH_N2	Manning's roughness for channels ($s{\cdot}m^{-1/3}$)	v	0.01–0.3	0.178 (0.175; 0.287)
ALPHA_BF	Baseflow recession constant (days)	v	0–1	0.3791 (0.367; 0.790)
ESCO	Soil evaporation compensation factor (-)	v	0–1	0.9879 (0.966; 1.000)

The parameters are ranked out by order of decreasing importance in the model. The units provided in the description stand for the absolute parameter value [Neitsch et al., 2011]. The calibration method refers to the strategy used for updating the model parameters during the calibration phase: r (for relative) is the relative deviation applied to the original parameter value, which therefore preserves its spatial variability; v (for replace) is the absolute and unique value given to the parameter in the model, regardless of its location [Abbaspour et al., 2007, Yonaba et al., 2021a].

the watershed response, a tendency in maximizing unused water (defined as P_{ex}) and unused energy (E_{ex}) occurs, as a depiction of the shift in ecohydrological signatures of the watershed. The direction of the change can therefore be explained in terms of: (i) increasing runoff or water stress (moving right or left along the P_{ex} axis, respectively); (ii) increased humidity or drier conditions (moving upward or downward along the E_{ex} axis, respectively). The excess water P_{ex} and excess energy E_{ex} are calculated as given by Equation (6):

$$\begin{cases} P_{\text{ex}} = \dfrac{P - \text{ET}_a}{P} \\ E_{\text{ex}} = \dfrac{\text{PET} - \text{ET}_a}{\text{PET}} \end{cases} \tag{6}$$

where, for each period, P is the average annual rainfall, ET_a is the average annual actual evapotranspiration and PET is the average annual potential evapotranspiration.

2.8. *Contributions of climate and land use changes to surface runoff*

The total relative change in average annual surface runoff signal between the baseline and the future (SSP2-4.5 and SSP5-8.5) is averaged over the climate model ensemble between the baseline period and the future SSP scenario considered, as shown in

Equation (7):

$$\Delta Q(\%) = \frac{1}{n}\sum_{i=M_1}^{M_n}\left(\frac{Q_{M_i,\mathrm{SSP}_j} - Q_b}{Q_b} \times 100\right) \quad (7)$$

where M_i, $i \in \{i,\ldots,n\}$ refers to each model within the ensemble, $n = 9$ is the total number of climate models used, Q_{M_i,SSP_j} refers to the average annual surface runoff in the future period under SSP_j ($j \in \{2\text{–}4.5 \text{ or } 5\text{–}8.5\}$) using climate model M_i, Q_b the average annual surface runoff during the baseline period.

As this total relative change is both affected by climate and land use change, the isolated contributions of each factor are evaluated using a "*fixing-changing*" method, where a single factor (either land use or climate) is changing [Yonaba et al., 2021a]. This needs intermediate simulations summarized in Table 3. The separation method however assumes that land use changes are independent of climate change, and the land-use change affects only actual evapotranspiration (ET). The latter assumption holds since actual ET is mostly dependent on vegetation (cover fraction, growing stage and development) and land use management [Dey and Mishra, 2017, Gbohoui et al., 2021, Yonaba et al., 2021a].

The relative contributions of climate (η_{climate}) and land use (η_{lulc}) changes to the total changes in surface runoff are evaluated under the assumption that these relative contributions, along with climate-land use interaction effects [Gbohoui et al., 2021, Yonaba et al., 2021a] sum up to 100%, as given in Equation (8).

$$\begin{cases} \eta_{\mathrm{climate}}(\%) + \eta_{\mathrm{lulc}}(\%) + \eta_{\mathrm{int}}(\%) = 100\% \\ \eta_{\mathrm{climate}}(\%) = \left(\frac{Q_{\mathrm{climate}} - Q_b}{Q_b}\right) \times 100 \\ \eta_{\mathrm{lulc}}(\%) = \left(\frac{Q_{\mathrm{lulc}} - Q_b}{Q_b}\right) \times 100 \\ \eta_{\mathrm{int}}(\%) = 100\% - \eta_{\mathrm{climate}}(\%) - \eta_{\mathrm{lulc}}(\%) \end{cases} \quad (8)$$

The same approach is used to disentangle climate and land use change contribution to changes in average annual surface runoff and also to changes in maximum daily surface runoff. In the latter case, however, Q_{climate} is defined as the ensemble median (instead of the average), since discrepancies across models within the ensemble become large with increasing return periods [Wallach et al., 2016].

3. Results

3.1. *Climate data processing*

3.1.1. *Calibration of HS model for daily PET*

The calibrated parameters of the Hargreaves–Samani equation for daily PET estimation is presented in Table 4, for each of the months in the year for which the formula is independently calibrated.

Figure 4 compares the distribution of daily PET values calculated with the reference Penman–Monteith (PM) model, the original HS model ($\mathrm{HS}_{\mathrm{raw}}$) and the calibrated HS model ($\mathrm{HS}_{\mathrm{calib}}$) over the period 1985–1994.

The $\mathrm{HS}_{\mathrm{raw}}$ values overestimate daily PM (Mann–Whitney: p-value <0.0001; RMSE = 1107 mm/d; PBIAS = −17.8%), whereas the calibrated $\mathrm{HS}_{\mathrm{calib}}$ values are closer in distribution to PM values, with non-significant differences in the mean (Mann–Whitney: p-value = 0.993; RMSE = 0.801 mm/d; PBIAS = −3.7%). The calibrated HS model is therefore expected to provide reliable estimates of daily PET in the Tougou watershed.

3.1.2. *Multivariate bias-correction of future climate data*

Figure 5 shows the cumulative distribution functions (CDF) of the 9 climate models selected in this study, compared to those of observations over the baseline period 1995–2014, before and after the application of the multivariate bias-correction *MBCn*.

The moderate to large discrepancies observed in CDFs (especially in rainfall) initially become marginal after the bias-correction, hence demonstrating the performance of the bias-correction method in adjusting the distributions for all the considered climatic variables. The transfer functions used for adjusting the historical climate model outputs were applied to the future forecasts (SSP2-4.5 and SSP5-8.5), hence providing more skilful climate projections.

3.2. *Analysis of the climate change signal*

3.2.1. *Projected changes in annual average rainfall and PET*

The climate change signal in SSP2-4.5 and SSP5-8.5 relative to the base line period is presented in Figure 6a. The majority of the climate models

Table 3. Simulation runs to isolate land use and climate change effects on surface runoff

Climate period	LULC period	Response	Description	Effect
Baseline	Baseline	Q_b	Runoff in the baseline period	-
Baseline	Future	Q_{lulc}	Changing land use while holding climate constant	Land use change
Future (ssp2-4.5, ssp5-8.5)	Baseline	Q_{climate}	Changing climate while holding LULC constant	Climate change
Future (ssp2-4.5, ssp5-8.5)	Future	Q_{future}	Runoff in the future period	Land use + Climate change

Table 4. Monthly calibrated parameters of Hargreaves–Samani equation for daily PET estimation in Tougou watershed

Parameters		J	F	M	A	M	J	J	A	S	O	N	D
k	Estimate	0.190	0.190	0.190	0.190	0.190	0.190	0.190	0.165	0.172	0.190	0.190	0.190
	Std. error	0.072	0.071	0.087	0.088	0.079	0.051	0.062	0.066	0.050	0.118	0.071	0.068
	p-value	0.009	0.008	0.030	0.031	0.017	0.000	0.002	0.014	0.001	0.108	0.008	0.006
n	Estimate	0.221	0.229	0.234	0.232	0.389	0.502	0.468	0.506	0.495	0.175	0.275	0.213
	Std. Error	0.056	0.060	0.052	0.045	0.072	0.066	0.071	0.077	0.053	0.051	0.059	0.056
	p-value	0.000	0.000	0.000	0.000	0.000	0.000	0.000	0.000	$<2\times10^{-16}$	0.001	0.000	0.000
b	Estimate	50.000	50.000	50.000	50.000	22.926	10.000	10.000	10.000	10.000	47.423	34.179	50.000
	Std. Error	22.127	24.905	37.118	38.718	19.677	8.571	9.325	11.486	8.176	47.241	20.293	20.984
	p-value	0.025	0.046	0.179	0.198	0.245	0.245	0.285	0.385	0.222	0.316	0.093	0.018
Residual error		0.648	0.781	0.967	0.895	1.114	1.010	0.846	0.816	0.591	0.609	0.592	0.576

within the ensemble project an increase in annual rainfall by 13.7% on average in SSP2-4.5 (−7.6% to 58.2%) and by 18.8% on average in SSP5-8.5 (−2.3% to 61.0%). Regarding annual PET, an increase is also expected by 1.3% on average in SSP2-4.5 (−0.2% to 2.5%) and by 1.5% on average in SSP5-8.5 (0.3% to 3.4%). The projected increase in PET is likely caused by the projected increase in temperatures.

An increase in monthly rainfall is expected (Figure 6b) for the months of June (17.6% and 14.3%), July (5.9% and 8.9%), August (13.7% and 20.8%) and September (15.8% and 26.5%), respectively under SSP2-4.5 and SSP5-8.5 scenarios. Similarly, for monthly PET, an increase is also projected, mostly for the warmest months of April (1.0% and 1.4%) and May (0.8% and 2.5%), but also for the rainy months of June (2.3% and 2.2%), July (1.7% and 2.0%) and August (1.7% and 0.9%).

3.2.2. *Projected changes in daily rainfall extremes*

Figure 7 shows the evolution of selected rainfall quantile projected by SSPs scenarios in comparison to the baseline period, for return periods of 2, 5, 10, 15, 20, 25 and 30 years. The projected rainfall extreme considered in this study are defined as the median of the GCM ensemble. The projected increase in rainfall quantiles is significant and is estimated at 26.6% to 45.1% (under SSP2-4.5) and 35.5% to 77.2% (under SSP5-8.5) over the different return periods.

3.3. *Projected changes on surface runoff*

3.3.1. *Annual changes*

The analysis of hydrological simulation outputs for the baseline and the future period reveals significant changes in average annual components of the watershed hydrological balance, as shown in

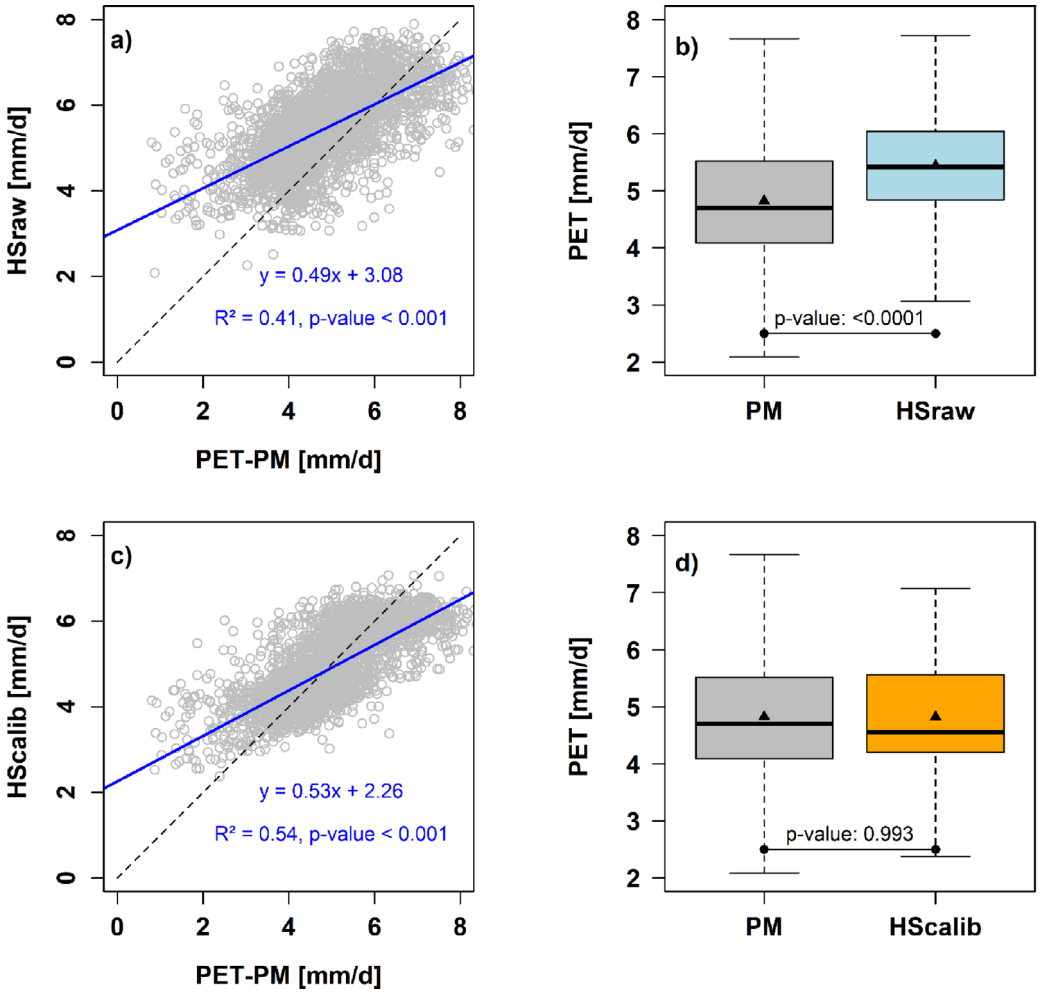

Figure 4. Comparison between PET estimates from Penman–Monteith (PM) reference method and Hargreaves–Samani (HS) equation over the period 1985–1994. Panels (a) and (b) compare PM and uncalibrated HS formula. Panels (c) and (d) compare PET estimates from PM and calibrated HS formula.

Figure 8. The increase in annual rainfall and PET is significant for both scenarios (p-value = 0.0032 and 0.0003 respectively). Furthermore, significant increase in surface runoff (SURQ) by 24.2% (SSP2-4.5: p-value = 0.0018) and by 34.3% (SSP5-8.5: p-value = 0.0001) is projected. Likewise, the annual runoff coefficient (RC) is also projected to increase significantly by 11.7% under SSP5-8.5 scenario (p-value = 0.0095).

The relative changes in annual rainfall and surface runoff reported for each climate model in the ensemble are presented in Figure 9. Under both SSPs, 8 climate models out of 9 (i.e. 89%) are projecting an increase in annual rainfall (Figure 9a) from 0.7% to 58.2% and from 6.6% to 61.0% (respectively under SSP2.4-5 and SSP5-8.5). Only 1 model (i.e. 11%) in the ensemble is projecting a decrease in rainfall of 7.6% (SSP2-4.5) and 2.3% (SSP5-8.5). Likewise, future average annual surface runoff (Figure 9b) is projected to increase under SSP2-4.5 (7 models, from 9.3% to 101.7%) and SSP5-8.5 scenarios (8 models, from 10.9% to 110.8%).

3.3.2. *Seasonal changes*

The seasonal changes in surface runoff in the Tougou watershed are presented in Figure 10, superimposed with changes in monthly rainfall. Under the

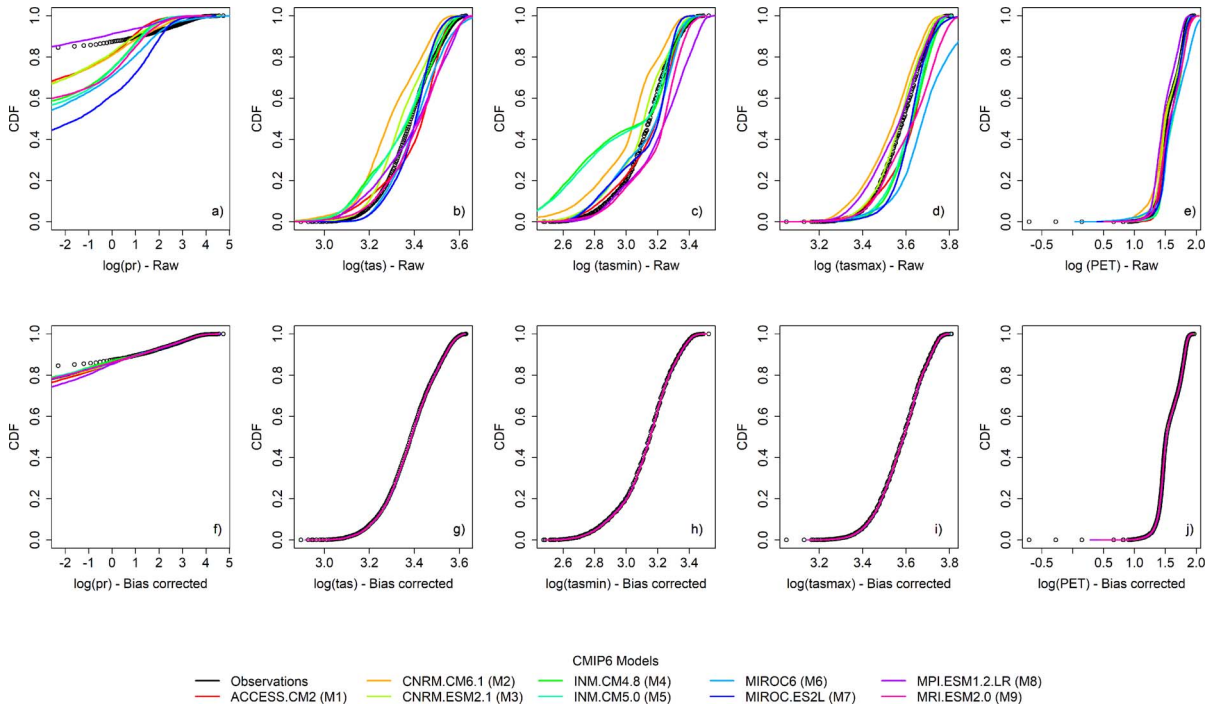

Figure 5. Cumulative distribution functions (CDFs) of climate variable before and after multivariate bias-correction over the baseline period 1995–2014. The x-axis scale for all panels were log-transformed to clearly visualize the differences in distributions (especially in rainfall).

SSP2-4.5 scenario (Figure 10a), surface runoff is projected to increase especially in the months of June (15.7 mm) and August (23.6 mm), resulting in a bimodal distribution of the projected increase. Under the SSP5-8.5 scenario (Figure 10b), the projected increase is rather unimodal, with a peak projected in August (35.4 mm), gradually decreasing in September (23.9 mm). It also appears that the reported increase in surface runoff appear to be driven by the increase in rainfall, which shows that rainfall is likely the prominent factor driving seasonal changes in surface runoff, further altered to a lesser extent by other external factors.

3.4. *Evolution of ecohydrological status*

The evolution of the ecohydrological status of the Tougou watershed is presented in Figure 11. The majority of the climate projections (8 models under SSP2-4.5, 7 models under SSP5-8.5) shows a shift to the right in terms of excess rainfall (P_{ex}), which translates as an increase in surface runoff under both SSP2-4.5 and SSP5-8.5 scenarios. However, in terms of aridity, less agreement is observed within the climate ensemble. A total of 4 models (out of 9) project a shift towards increased aridity or drier conditions (increase in excess energy E_{ex}), whereas 5 models project a shift towards more humid conditions (decrease in excess energy E_{ex}). The direction of the shift for the majority of the models in terms of (E_{ex}) (in the positive $P_{ex} - E_{ex}$ quadrant) suggests changes in land use such as deforestation, removal of perennials or the use of conservation tillage [Tomer and Schilling, 2009], which is in line with the future land use maps in the Tougou watershed (increase in agricultural areas, decrease of natural vegetation).

However, it should be critically assumed that such picture of the ecohydrological evolution of the Tougou watershed does not quantify streamflow change, but rather provide qualitative insights regarding whether the reported change is mostly driven by climate or land use [Dey and Mishra, 2017].

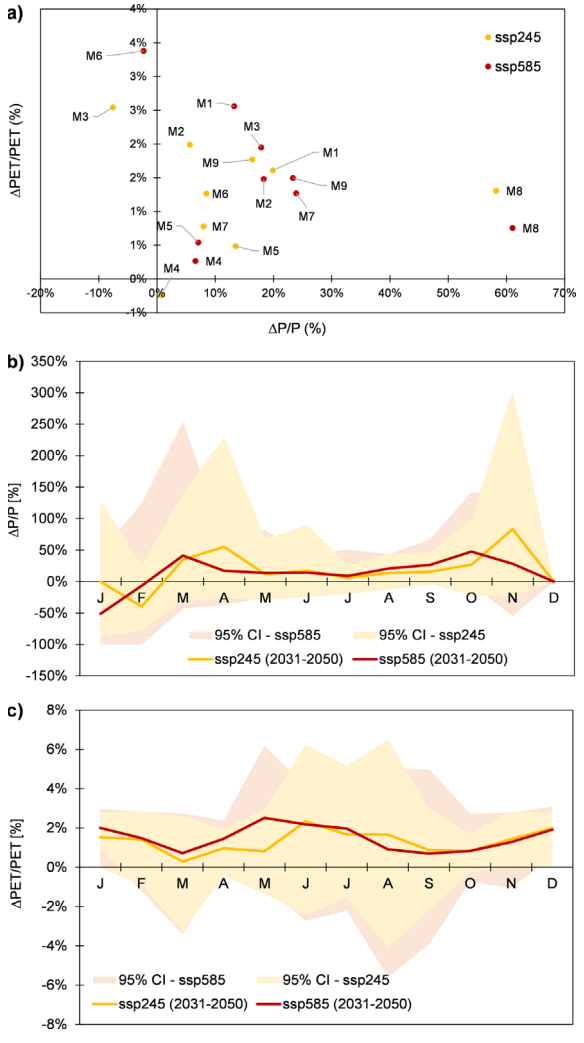

Figure 6. Annual and seasonal climate change signal in rainfall and PET relative to the baseline period 1995–2014. (a) Relative change in annual rainfall and PET. (b) Relative change in monthly rainfall. (c) Relative changes in monthly PET.

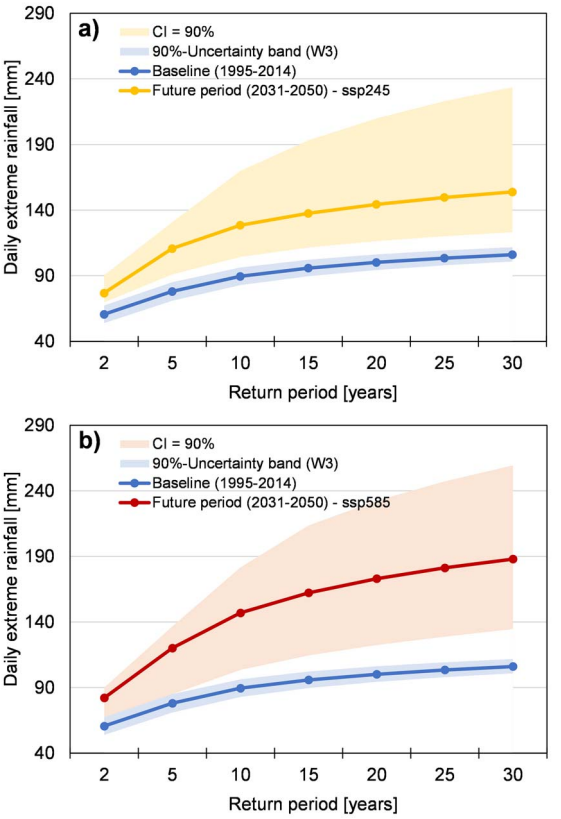

Figure 7. Projection of daily annual rainfall extremes in baseline (1995–2014) and future (2031–2050) periods. (a) Median projection under SSP2-4.5 scenario. (b) Median projection under SSP5-8.5 scenario. The shaded areas in light yellow and light orange represent the 90% uncertainty band around the median projections across the GCM ensemble. The blue shaded area refers to the 90% uncertainty band around Weibull-3 (W3) quantiles over the baseline period.

3.5. *Evolution of surface runoff*

3.5.1. *Sensitivities of surface runoff to rainfall and PET*

The sensitivities of annual runoff change to rainfall and PET change under SSPs scenarios are presented in Figure 12 for all climate models in the ensemble used in this study. Such sensitives, commonly referred to as streamflow elasticity, describes the change in streamflow related the changes in one climate variable [Andréassian et al., 2016]. In this study, the analysis reveals that in the Tougou watershed, the change in surface runoff is not significantly affected by changes in annual PET (Figure 12a), as shown by the very small coefficients of determination (SSP2-4.5: $R^2 = 0.0002$, p-value = 0.973; SSP5-8.5: $R^2 = 0.1519$, p-value = 0.300). However, rainfall appears as the major factor driving changes in annual surface runoff (SSP2-4.5: $R^2 = 0.9949$, p-value <

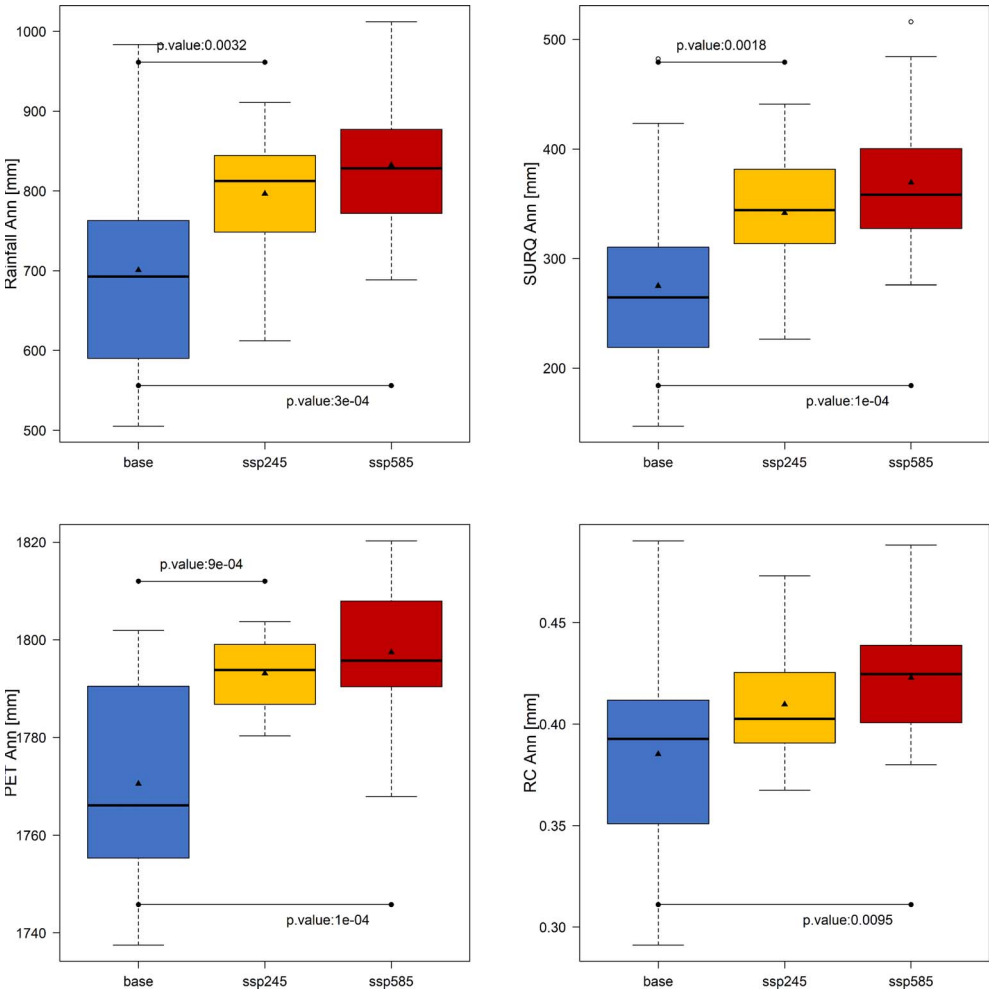

Figure 8. Comparison of annual changes in hydrological processes in the Tougou watershed. PET: potential evapotranspiration. SURQ: surface runoff. RC: runoff coefficient, calculated as RC = SURQ/Rainfall.

0.0001; SSP5-8.5: $R^2 = 0.9928$, p-value < 0.0001), following a linear relationship (Figure 12b). Moreover, it can be inferred from Figure 12b that the projected average annual elasticity of streamflow to rainfall under SSP2-4.5 scenario is 0.69 (ratio of average annual increase of 66.6 mm in surface runoff out of 95.8 mm in rainfall). This elasticity increases to 0.72 under SSP5-8.5 scenario (ratio of average annual increase of 94.2 mm in surface runoff out of 131.6 mm in rainfall).

3.5.2. *Changes in daily Flow Duration Curve (FDC)*

The changes in daily flow duration curves (FDC) during the rainy season (June to October) in the Tougou watershed are presented in Figure 13. The analysis shows that an increase in daily surface runoff is expected under both SSPs scenarios. For instance, Q_{10} (surface runoff equalled or exceeded 10% of the time) increases from 4.0 mm (baseline) to 4.2 mm (SSP2-4.5) or 4.6 mm (SSP5-8.5). Also, Q_{50} (surface runoff equalled or exceeded 50% of the time) increases from 1.2 mm (baseline) to 2 mm (under both SSPs). Likewise, Q_{80} (surface runoff equalled or exceeded 80% of the time) increases from 0.35 mm (baseline) to 0.70 mm (SSP2-4.5) or 0.80 (SSP5-8.5). The observed increase in FDC suggest and shift towards an intensification of flow regimes, likely driven by the intensification in the rainfall over the Tougou

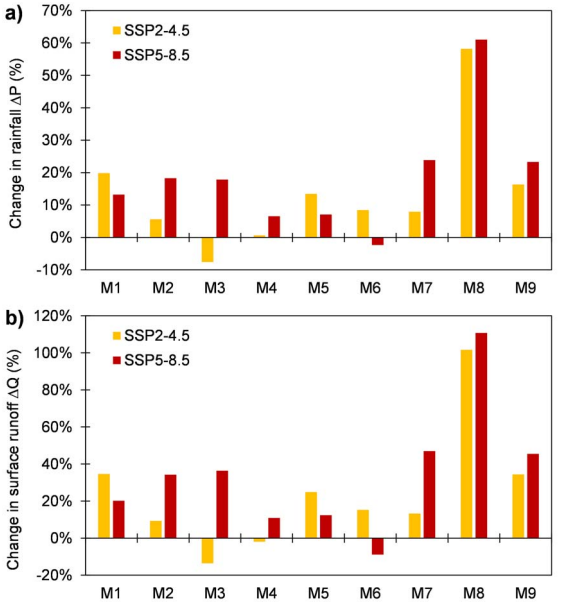

Figure 9. Relative average annual changes in rainfall (a) and surface runoff (b) between the baseline (1995–2014) and the future (2031–2050) period under SSP2-4.5 and SSP5-8.5 scenarios.

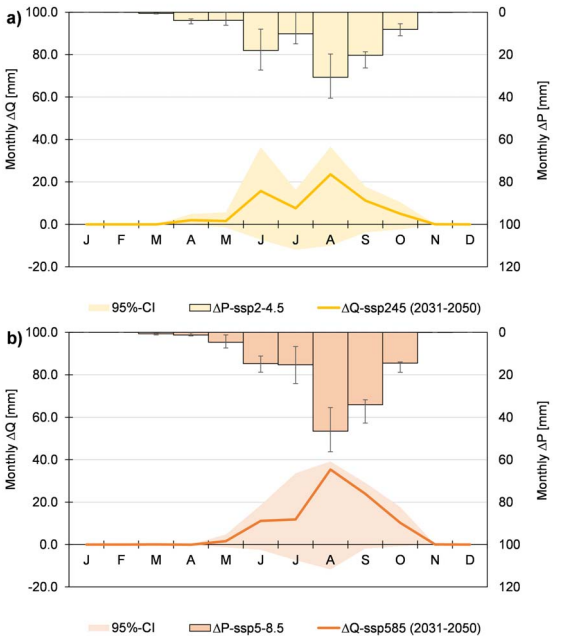

Figure 10. Monthly projected changes in surface runoff in the Tougou watershed. (a) Under SSP2-4.5 scenario. (b) Under SSP5-8.5 scenario. The error bars on rainfall and the yellow and orange grey bands shows the 95% confidence interval around projected, calculated from the ensemble values.

watershed.

3.6. *Effects of climate and land use changes on surface runoff*

3.6.1. *Contribution of climate and land use to changes in annual surface runoff*

The isolated relative contributions of climate and land use changes to annual surface runoff are presented in Figure 14, averaged over the period 2031–2050. Figures 14a and c shows the relative contribution of climate and land use for the specific case where surface runoff is projected to increase (respectively under SSP2-4.5 and SSP5-8.5 scenarios). At the opposite, Figures 14b and d shows the relative contribution of climate and land use for the specific case where surface runoff is projected to decrease (respectively under SSP2-4.5 and SSP5-8.5 scenarios). For all panels in Figure 14, a positive (or relative) contribution translates that the projected changes in the factor (climate or land use) tends to cause an increase (or a decrease) in surface runoff.

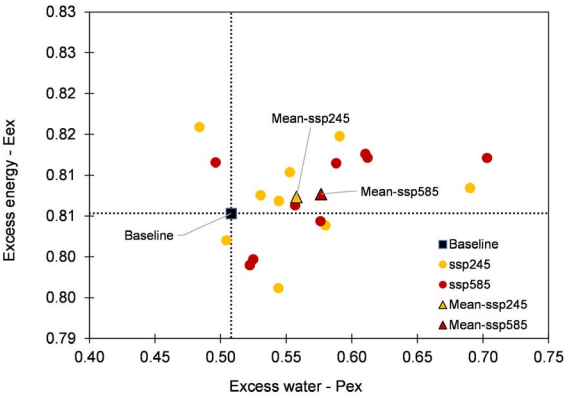

Figure 11. Projected shifts in the ecohydrological status of the Tougou watershed.

Under SSP2-4.5 scenario, surface runoff is projected to increase (between 25.7 mm and 279.6 mm) for 7 climate models (Figure 14a), which are the wetter ones (increase in average annual rainfall

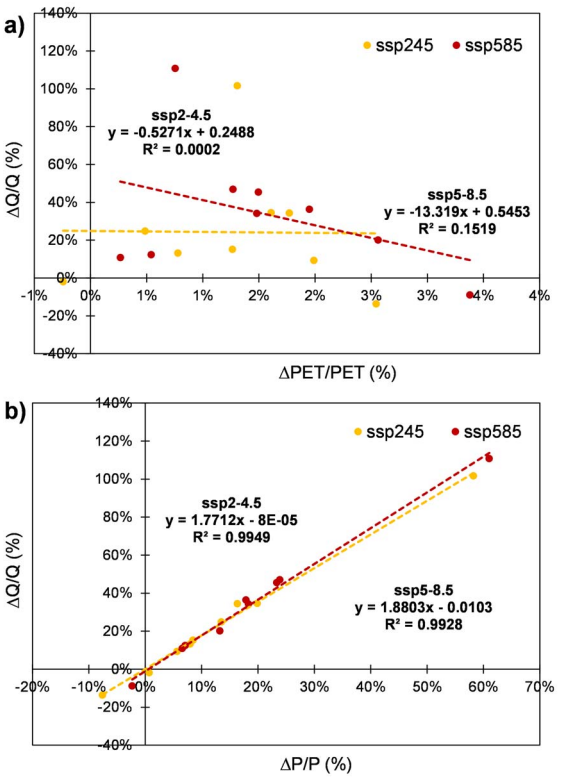

Figure 12. Sensitivities of annual surface runoff to rainfall and PET across all climate models in the ensemble of 9 models. Each dot shows the relative change in annual average for a given climate model between the baseline (1995–2014) and the future period (2031–2050).

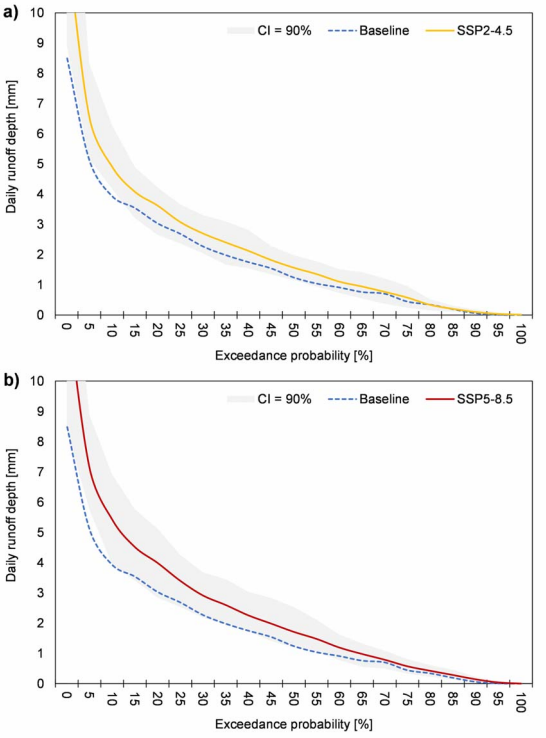

Figure 13. Projected changes in flow duration curve (FDC) in the Tougou watershed. (a) Changes in FDC under SSP2-4.5 scenario. (b) Changes in FDC under SSP5-8.5 scenario. The grey shaded area represents the 90%-confidence interval around the FDC curves for both scenarios.

projected between 5.6% and 58.2%). In contrast (Figure 14b), for the 2 remaining drier climate models M3 and M4 (average annual rainfall change projected between −7.6% and 0.7%), surface runoff is projected to decrease (between 2.3 and 37.5 mm). When surface runoff is projected to increase (Figure 14a), the relative contributions of climate and land use to such increase range from 109.0% to 170.7% and from −6.6% to −71.5% respectively. When surface runoff is projected to decrease (Figure 14b), these relative contributions now range from −246.9% to 55.3% and from 48.9% to 349.3%. In this case, the model M4 shows a positive contribution as it projects a small rainfall increase (0.7%), which tends to increase surface runoff, albeit this contribution appears minor in comparison to the land use effect (which consistently tends to decrease surface runoff).

Under SSP5-8.5 scenario, the projected figures are similar: for 8 climate models in the ensemble (Figure 14c), surface runoff is projected to increase (between 29.9 mm and 304.7 mm). These 8 climate models are mostly wet (average annual rainfall increase projected between 6.6% and 61.0%). The relative contributions of climate and land use to the projected increase in surface runoff range from 108.0% and 160.9% and from −6.0% to −61.3% respectively. For the remaining drier climate model, M6 (projecting a decrease in annual rainfall of 2.3%), the annual surface runoff is projected to decrease by 24.4 mm: the relative contributions of climate and land use to this decrease are of 26.3% and 75.2% respectively (Figure 14d).

Overall, it appears that the relative contribution of climate is dominant under both SSP2-4.5 and

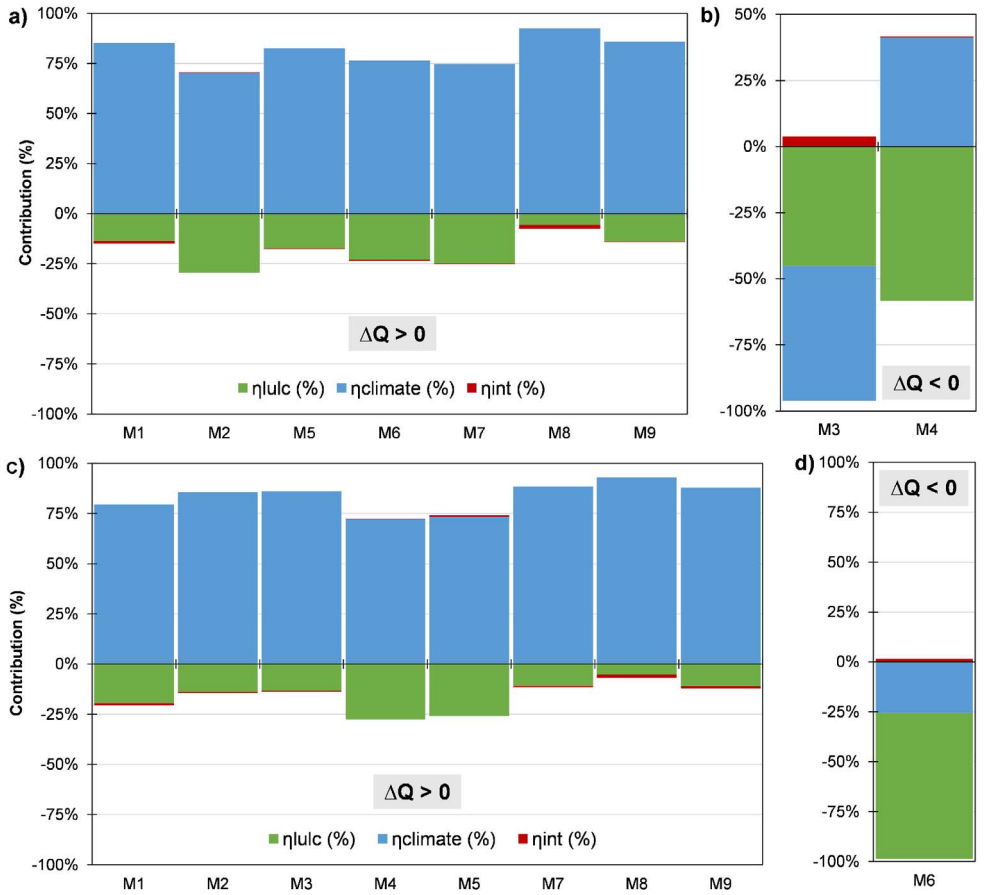

Figure 14. Average relative contributions of climate (η_{climate}) and land use (η_{lulc}) to changes in average annual surface runoff between the baseline (1995–2014) and future (2031–2050) periods in Tougou watershed. (a) SSP2-4.5 scenario, surface runoff projected to increase. (b) SSP2-4.5 scenario, surface runoff projected to decrease. (c) SSP5-8.5 scenario, surface runoff projected to increase. (d) SSP5-8.5 scenario, surface runoff projected to decrease. η_{int} refers to the average relative contribution of interaction effects between climate and land use.

SSP5-8.5 scenarios, as it is on absolute average 1.1 to 16.6 times higher (under SSP2-4.5) and 2.6 to 17.9 times higher (under SSP5-8.5) than that of land use. The increase in surface runoff could mainly be attributed to the increase in rainfall, further lessened by the effect of land use changes which typically tends to decrease surface runoff under all scenarios. The decrease in surface runoff can be explained by the decrease in bare areas between the baseline and the future period (from 44.8% to 10.7%). This decrease tends to produce less surface runoff. These bare areas are further replaced by cropland (which increased from 48.6% to 86.6%); these croplands tends to produce less surface runoff than bare areas [Yonaba et al., 2021a].

Smaller residual contributions, which range from −4.2% to 0.7% and from −2.0% to 1.6% under SSP2-4.5 and SSP5-8.5 respectively can be attributed to climate-land use interactions effects on surface runoff. Such contribution appears to be relatively small at the scale of the Tougou watershed. However, it should be acknowledged that these contributions convey various forms of uncertainties [Gbohoui et al., 2021, Onyutha et al., 2021, Yonaba et al., 2021a].

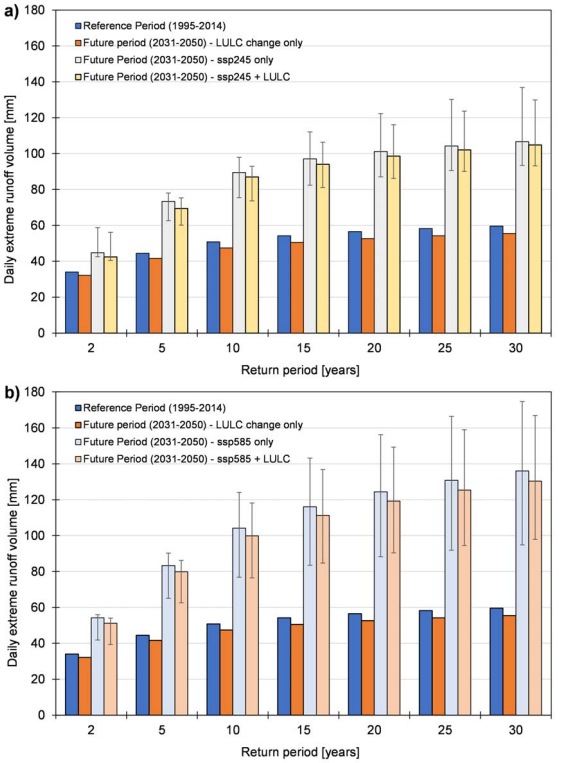

Figure 15. Projected changes in maximum surface runoff quantiles under climate and land use changes. (a) Changes under SSP2-4.5 scenario. (b) Changes under SSP5-8.5 scenario. The error bars delineate the 90% confidence interval around the estimates across the models in the GCM ensemble.

3.6.2. *Contribution of climate and land use to changes in maximum daily surface runoff*

The Figure 15 pictures the evolution of daily maximum surface runoff for return periods from 2 to 30 years, under various scenarios (climate change, land use change). The quantification of these changes is presented in Table 5. A total increase in maximum daily surface runoff (SSP2-4.5: 8.4 mm to 45. 2 mm; SSP5-8.5: 17.1 mm to 70.8 mm) is projected. The analysis reveals that land use change causes of a decrease in maximum daily surface runoff (SSP2-4.5: $\eta_{\text{lulc}} = -22.8\%$ to -9.1%; SSP5-8.5: $\eta_{\text{lulc}} = -11.1\%$ to -5.8%). Also, the absolute reduction induced by land use changes decreases for increasing return periods. At the opposite, climate change causes an increase in maximum daily surface runoff (SSP2-4.5: $\eta_{\text{climate}} = 127.2\%$ to 104.0%; SSP5-8.5: $\eta_{\text{climate}} = 117.7\%$ to 108.0%). Climate-land use interactions effects are also quantified (SSP2-4.5: $\eta_{\text{int}} = -4.4\%$ to 5.1%; SSP5-8.5: $\eta_{\text{int}} = -6.5\%$ to 2.1%), although being relatively small in comparison to the isolated impact of climate and land-use changes. In definitive, the projected contributions of climate and land use on maximum daily surface runoff are similar to those observed on average annual values, albeit larger in magnitude.

4. Discussion

4.1. *On the contributions of climate and land use changes to surface runoff*

In this study, using a hydrological modelling framework, the combined and isolated impact of climate and land use changes on surface runoff have been assessed between a baseline period 1995–2014 and a future period 2031–2050, under two warming scenarios (SSP2-4.5 and SSP5-8.5). The overall analysis results showed that rainfall and PET are projected to increase (under both SSPs), which is likely to cause an increase in actual evapotranspiration as well. Furthermore, the increase in rainfall is likely causing an increase in surface runoff, overriding the minor streamflow reduction caused by land use changes.

In previous studies, the hydrological response of West African watersheds to changes in climate and land use have been reported for past (historical) and current conditions. Many studies established that surface runoff generating mechanisms in the Sahel region are tightly dependent on soil surface conditions, hence explaining the dominant effect of land use changes over past and current climate conditions on changes in hydrological balance [Descroix et al., 2018, Gal et al., 2017, Karambiri et al., 2011, Paturel et al., 2017, Séguis et al., 2004, Yonaba et al., 2021a]. Yet, few studies have assessed the specific contributions of climate and land use changes on surface runoff variability and changes in West Africa.

Aich et al. [2015] used the Soil and Water Integrated Model (SWIM) with dynamic land use update to assess the relative contributions of climate and land use to the change in trends in floods magnitude. Without drawing a general answer, roughly

Table 5. Isolated contributions of climate and land use to changes in daily surface runoff quantiles

Future scenario		Q_2	Q_5	Q_{10}	Q_{15}	Q_{20}	Q_{25}	Q_{30}
SSP2-4.5	ΔQ_t (mm)	8.4	25.0	36.2	39.8	42.1	43.8	45.2
	ΔQ_{lulc} (mm)	−1.9	−2.8	−3.4	−3.7	−3.9	−4.0	−4.1
	$\Delta Q_{\text{climate}}$ (mm)	10.7	28.9	38.6	42.8	44.7	46.0	47.1
	η_{lulc} (%)	−22.8%	−11.3%	−9.3%	−9.2%	−9.2%	−9.2%	−9.1%
	η_{climate} (%)	127.2%	115.8%	106.7%	107.6%	106.1%	105.0%	104.0%
	η_{int} (%)	*−4.4%*	*−4.5%*	*2.7%*	*1.7%*	*3.1%*	*4.2%*	*5.1%*
SSP5-8.5	ΔQ_t (mm)	17.1	35.4	49.0	57.1	62.8	67.2	70.8
	ΔQ_{lulc} (mm)	−1.9	−2.8	−3.4	−3.7	−3.9	−4.0	−4.1
	$\Delta Q_{\text{climate}}$ (mm)	20.2	38.9	53.4	61.9	67.9	72.6	76.5
	η_{lulc} (%)	−11.1%	−8.0%	−6.9%	−6.4%	−6.2%	−6.0%	−5.8%
	η_{climate} (%)	117.7%	109.8%	108.8%	108.5%	108.2%	108.1%	108.0%
	η_{int} (%)	−6.5%	−1.8%	−2.0%	−2.0%	−2.1%	−2.1%	−2.1%

Q_2 refers to the daily extreme surface runoff for 2-years return period. Likewise, Q_{30} is the daily extreme surface runoff for a 30-years return period. ΔQ_t is the total change in surface runoff affected both by climate and land use changes. ΔQ_{lulc} is the change in surface runoff caused by land use change, and $\Delta Q_{\text{climate}}$ is the change in surface runoff caused by climate change.

equal shares of contributions for land use and climate contributions are reported for Gorouol and Sirba catchments. Sidibe et al. [2019] showed that in most of the West African Sahel, changes in land use are the major driver in surface runoff fluctuations over the period 1950–1990, further amplified by climate variability that occurred within the same period. Yonaba et al. [2021a] used the SWAT model in the Tougou watershed, over the historical period 1952–2005 and found that the fluctuations in surface runoff along with the hydrological paradox that occurred within the 1970s (likewise, in most Sahelian hydrosystems) could mainly be attributed to land use changes. Gbohoui et al. [2021], in the Nakanbe River Basin, reported similar conclusions using a Budyko-type separation approach; however, the same authors observed an increasing contribution of climate-environment interaction effects on surface runoff fluctuations.

Regarding future climate projections over the Sahel area, essentially for rainfall, forecasts are mitigated, with high zonal contrasts. For the 2050 timeline, Mbaye et al. [2016] projected a decrease in rainfall over the western part of the Sahel; Tazen et al. [2013] projected a change in annual rainfall in the range of −3% to +10% over the Nakanbe River Basin; Badou et al. [2018] reported an increase in rainfall (1.7% to 23.4%), but with contrasting changes (−8.5% to 17.3%) over the Niger River basin. Recently, Dieng et al. [2022] projected a significant increase in rainfall between 5% to 20% for Sahara and Western Sahel regions using bias-corrected high-resolution climate change simulations. Ultimately, there is still no consensus across studies on the direction in which rainfall is likely to evolve over the West African Sahel [Almazroui et al., 2020], let alone the resulting impacts on hydrological processes [Stanzel et al., 2018]. Also, large uncertainties across climate models are still persistent, bringing a supplemental layer of complexity in assessing future forecasts [Hattermann et al., 2018, Laux et al., 2021]. It should also be acknowledged that most of the previous studies use datasets issued from CMIP5 models. In this regard, this study sheds new insights in comparison, as it is among the first (to the best of our knowledge) to assess the latest available iteration of climate change simulations, that is CMIP6, in northern Burkina Faso.

In terms of future projections, this study reported an increase in surface runoff, more likely controlled by an increase in rainfall, although slightly mitigated by future land use changes. The dominant control of climate (i.e. rainfall) expected in the future

is clearly at the opposite of what occurred in past and current conditions, and is likely attributable to: (1) the large increase in rainfall conditions; (2) the almost exclusive sensitivity of surface runoff to rainfall conditions; (3) the scale of observation which is, in this study, relatively small (37 km^2). As shown in Mounirou et al. [2020, 2021], surface runoff generating processes change with scale. Likewise, Gbohoui et al. [2021] showed that for varying nested watersheds scale, the control of environmental conditions (i.e., land use) is dependent on the size of the watershed. In contrast for example, in southwestern Burkina Faso, Idrissou et al. [2022] projected to the 2050 horizon an increase in surface runoff (12% to 95%) and also a decrease (24% to 44%), primarily driven by land use changes in both cases.

Regarding annual maximum surface runoff, an increase in the amplitude of runoff quantiles is reported in this study, largely caused by the increase in rainfall quantiles. These findings agree with previous studies, which reported an intensification of rainfall over the Sahel region, with a subsequent increase in surface runoff in most of the cases [Panthou et al., 2018, Taylor et al., 2017, Tazen et al., 2019, Tramblay et al., 2020]. Hounkpè et al. [2019] showed that land use changes (especially the conversion of natural vegetation to croplands) could contribute to the increase in both the frequency and magnitude of floods, amplifying the contribution of the projected rainfall increase.

4.2. *Practical implications of this study*

In the light of the findings presented in this study, a few major practical implications to hydrologists and water resource managers can be drawn:

(1) there is a need to assess, at larger and various scales and contexts, the direction of the future evolution of climate based on future climate projections. Yet, the cautious use of such data in impact studies is recommended, since they can be fraught with large discrepancies with past observations over their historical baselines [Dieng et al., 2022]. Post-processing these simulations is always possible (bias-correction), even though the added value of such processing is questionable, and should be critically discussed depending on the impact study to be carried out [Laux et al., 2021]. This also relates to the need for large sets of observations, which are scarce in the Sahelian context. Gridded datasets [Dembélé et al., 2020, Satgé et al., 2020], which provide estimations of rainfall from satellite observations, or bottom-up inversion from soil humidity [Brocca et al., 2019, Yonaba et al., 2022] can be considered as reliable alternatives.

(2) There is also a growing need to include hydrological modelling at the core of water resource management. With the increase of available hydrological models of varying complexity, interesting insights can be drawn regarding how various processes and inputs affects a watershed balance, and therefore developing informed strategies for water resource management can be further considered [Karambiri et al., 2011, Lèye et al., 2021].

(3) Also, regarding hydrological modelling, it is established that land use changes significantly affect surface runoff, especially in the Sahel region. Yet, in its current practice, most hydrological modelling applications still represent land use with static conditions, which leads to either inaccurate representation of spatial/temporal patterns of hydrological processes, or over/under parametrization of such models [Hounkpè et al., 2019, Wagner et al., 2016, Yonaba et al., 2021a]. Therefore, there is a need to develop integrated modelling frameworks, to fully account for dynamic land use changes during hydrological simulations, for more reliable outputs.

4.3. *Limitations of this study*

Some of the limitations this study is fraught with should be acknowledged, to clarify the scope to which the reported results should be fully assessed.

First, for future rainfall projections, only the mean (or the median) of the model ensemble was considered most of the time, which is valid since the ensemble features a large number of models [Maraun, 2016]. However, an in-depth assessment of the uncertainty range around future projections should be carried out to draw a more complete picture of the possible contribution of climate change and land use to changes in surface runoff. In this

study for example, uncertainties stem from multiple sources, including the GCM selection, the climate data pre-processing (statistical bias-correction), the land use/land cover maps (which embody spatial and structural uncertainties) and the hydrological model parametrization and simulations. The issue is acute in general to all impact studies which use a hydro-climatic modelling chain to assess the contributions of climate and land use on the water resource [Clark et al., 2016]. In this study, in an effort to bridge this gap, uncertainties around GCM projections in rainfall and surface runoff are provided to some extent, based on aggregation of the individual models in the GCM ensemble. However, the uncertainty range around the hydrological model parameters range was not fully assessed on surface runoff estimates. However, dedicated research paths are proposing explicit approaches to decompose uncertainties (i.e. variance decomposition) according to its various sources to provide a better quantitative and qualitative insight regarding how trustful the projected impacts should be perceived [Bosshard et al., 2013, Gao et al., 2019].

Second, regarding future land use, a single business-as-usual narrative, was considered in this study [Yonaba et al., 2021b]. This trajectory is actually closely similar to the land use narrative built within SSP2-4.5 [Popp et al., 2017]. However, different land change scenarios should be assessed through the framework used in this study, to provide a larger picture of the contribution of various land use narratives on surface runoff in the study area. Such future land use maps can be developed using statistical pattern-based approaches (cellular automata or artificial neural networks, for example), coupled with land demand models build around future scenarios: expansion of croplands to meet increasing food demand, mitigation policies to preserve natural vegetation for sustainability, etc. [Yonaba et al., 2021b].

5. Conclusion

This study seeks to quantify the contribution of climate and land use to changes in surface runoff in the Tougou watershed, a typical Sahelian hydrosystem, located in the Upper Nakanbe River basin, in Burkina Faso (in West Africa). Between the baseline period (1995–2014) and the future period (2031–2050), a multi-model ensemble of 9 GCMs (issued from CMIP6 simulations) is used to drive a calibrated hydrological SWAT model, along with a dynamic land use update of LULC maps (for past and future conditions). An increase in annual rainfall (13.7% and 18.8%, respectively under SSP2-4.5 and SSP5-8.5 scenarios) and also in daily maximum rainfall (from 26.6% to 45.1% under SSP2-4.5 and from 35.5% to 77.2% under SSP5-8.5 scenarios), is projected. This increase is found to be the major cause of a significant increase in daily surface runoff, as shown by the rise of flow duration curve. The annual streamflow is projected to increase (24.2% and 34.3% under SSP2-4.5 and SSP5-8.5 respectively). In terms of relative contributions, land use change (mainly the conversion of bare lands to croplands) is expected to cause a decrease in annual surface runoff, with a contribution of −27.6% to −19.5% (under SSP2-4.5 and SSP5-8.5 scenarios respectively), and also in maximum daily surface runoff (SSP2-4.5: −22.8% to −9.1% and SSP5-8.5 11.1% to −5.8%). In contrast, the contribution of climate (i.e., the rainfall) to the annual surface runoff increase is dominant, with a contribution of +128.8% and +120.7% (respectively under SSP2-4.5 and SSP5-8.5 scenarios), and likewise for maximum daily surface runoff (SSP2-4.5: +127.2% to +104.0%; SSP5-8.5: +117.7% to +108.0%).

Overall, these results shed light on the isolated contributions of climate and land use, and their interaction to the changes in hydrological processes. It also shows that such processes stem from the complex nature and interplay between climate and land change (both including natural and anthropogenic change), which should be fully assessed and integrated within an integrated modelling framework for more realistic and more reliable outputs. Finally, as the increase in surface runoff in the Tougou watershed is likely, future strategies should focus on: (i) mitigation of associated risks such as flood control; (ii) surface runoff management through farming practices (zaï, half-moons, stone rows) to increase soil water content for agricultural production; (ii) and finally, mitigation of runoff erosion. The results of this study might significantly help in framing such policies, as it unveils increased risks relating to climate change in the future, which could be effectively mitigated through local and effective land use decisions.

Conflicts of interest

Authors have no conflict of interest to declare.

Acknowledgements

This study has been carried out under the financial support of the Work Bank, through the Government of Burkina Faso (grant IDA n° 5420-BF). The authors are also extremely grateful to the local community of the Tougou village (in Burkina Faso) for their helpful assistance and cooperation; especially since this local community is nowadays hardly affected by the ongoing security crisis in Burkina Faso.

References

Abbaspour, K. C., Vejdani, M., Haghighat, S., and Yang, J. (2007). SWAT-CUP calibration and uncertainty programs for SWAT. In *MODSIM 2007 International Congress on Modelling and Simulation, Modelling and Simulation Society of Australia and New Zealand*, pages 1596–1602.

Aghsaei, H., Mobarghaee Dinan, N., Moridi, A., Asadolahi, Z., Delavar, M., Fohrer, N., and Wagner, P. D. (2020). Effects of dynamic land use/land cover change on water resources and sediment yield in the Anzali wetland catchment, Gilan, Iran. *Sci. Total Environ.*, 712, article no. 136449.

Aich, V., Liersch, S., Vetter, T., Andersson, J., Müller, E., and Hattermann, F. (2015). Climate or land use?—Attribution of changes in river flooding in the sahel zone. *Water*, 7, 2796–2820.

Akoko, G., Le, T. H., Gomi, T., and Kato, T. (2021). A review of SWAT model application in Africa. *Water*, 13, article no. 1313.

Almazroui, M., Saeed, F., Saeed, S., Nazrul Islam, M., Ismail, M., Klutse, N. A. B., and Siddiqui, M. H. (2020). Projected change in temperature and precipitation over Africa from CMIP6. *Earth Syst. Environ.*, 4, 455–475.

Amogu, O., Esteves, M., Vandervaere, J.-P., Malam Abdou, M., Panthou, G., Rajot, J.-L., Souley Yéro, K., Boubkraoui, S., Lapetite, J.-M., Dessay, N., Zin, I., Bachir, A., Bouzou Moussa, I., Faran Maïga, O., Gautier, E., Mamadou, I., and Descroix, L. (2015). Runoff evolution due to land-use change in a small Sahelian catchment. *Hydrol. Sci. J.*, 60, 78–95.

Andréassian, V., Coron, L., Lerat, J., and Le Moine, N. (2016). Climate elasticity of streamflow revisited—an elasticity index based on long-term hydrometeorological records. *Hydrol. Earth Syst. Sci.*, 20, 4503–4524.

Angelina, A., Gado Djibo, A., Seidou, O., Seidou Sanda, I., and Sittichok, K. (2015). Changes to flow regime on the Niger River at Koulikoro under a changing climate. *Hydrol. Sci. J.*, 60, 1709–1723.

Arnold, J., Srinivasan, R., Muttiah, R. S., and Williams, J. R. (1998). Large area hydrologic modeling and assessment Part I: model development. *J. Am. Water Res. Assoc.*, 34, 73–89.

Ayugi, B., Jiang, Z., Iyakaremye, V., Ngoma, H., Babaousmail, H., Onyutha, C., Dike, V. N., Mumo, R., and Ongoma, V. (2022). East African population exposure to precipitation extremes under 1.5 °C and 2.0 °C warming levels based on CMIP6 models. *Environ. Res. Lett.*, 17(4), article no. 044051.

Badou, D. F., Diekkrüger, B., Kapangaziwiri, E., Mbaye, M. L., Yira, Y., Lawin, E. A., Oyerinde, G. T., and Afouda, A. (2018). Modelling blue and green water availability under climate change in the Beninese Basin of the Niger River Basin, West Africa. *Hydrol. Process.*, 32, 2526–2542.

Belemtougri, A. P., Ducharne, A., Tazen, F., Oudin, L., and Karambiri, H. (2021). Understanding key factors controlling the duration of river flow intermittency: Case of Burkina Faso in West Africa. *J. Hydrol.: Reg. Stud.*, 37, article no. 100908.

Bhagat, S. K., Tiyasha, T., Al-khafaji, Z., Laux, P., Ewees, A. A., Rashid, T. A., Salih, S., Yonaba, R., Beyaztas, U., and Yaseen, Z. M. (2022). Establishment of dynamic evolving neural-fuzzy inference system model for natural air temperature prediction. *Complexity*, 2022, article no. 1047309.

Biasutti, M. (2019). Rainfall trends in the African Sahel: Characteristics, processes, and causes. *Wiley Interdiscip. Rev.: Clim. Change*, 10, article no. e591.

Bosshard, T., Carambia, M., Goergen, K., Kotlarski, S., Krahe, P., Zappa, M., and Schär, C. (2013). Quantifying uncertainty sources in an ensemble of hydrological climate-impact projections: uncertainty sources in climate-impact projections. *Water Resour. Res.*, 49, 1523–1536.

Brocca, L., Filippucci, P., Hahn, S., Ciabatta, L., Massari, C., Camici, S., Schüller, L., Bojkov, B., and Wagner, W. (2019). SM2RAIN–ASCAT (2007–2018): global daily satellite rainfall data from ASCAT soil

moisture observations. *Earth Syst. Sci. Data*, 11, 1583–1601.

Cannon, A. J. (2018). Multivariate quantile mapping bias correction: an N-dimensional probability density function transform for climate model simulations of multiple variables. *Clim. Dyn.*, 50, 31–49.

Cannon, A. J., Sobie, S. R., and Murdock, T. Q. (2015). Bias correction of GCM precipitation by quantile mapping: how well do methods preserve changes in quantiles and extremes? *J. Clim.*, 28, 6938–6959.

Clark, M. P., Wilby, R. L., Gutmann, E. D., Vano, J. A., Gangopadhyay, S., Wood, A. W., Fowler, H. J., Prudhomme, C., Arnold, J. R., and Brekke, L. D. (2016). Characterizing uncertainty of the hydrologic impacts of climate change. *Curr. Clim. Change Rep.*, 2, 55–64.

Connors, S., Dionne, M., Hanak, G., Musulin, R., Aellen, N., Amjad, M., Bowen, S., Carrascal, D. R., Coppola, E., Moro, E. D., Dosio, A., Faria, S. H., Gan, T. Y., Gomis, M., Gutierrez, J. M., Hope, P., Kopp, R., Krakovska, S., Leitzell, K., Maraun, D., Masson-Delmotte, V., Matthews, R., Maycock, T., Paddam, S., Plattner, G.-K., Pui, A., Rahimi, M., Ranasinghe, R., Rogelj, J., Ruane, A. C., Szopa, S., Turner, A., Vautard, R., Velichkova, Y., Weigel, A., and Zhang, X. (2022). *Climate Science: A Summary for Actuaries—What the IPCC Climate Change Report 2021 Means for the Actuarial Profession (Report)*. International Actuarial Association, Ottawa, Canada.

Cornelissen, T., Diekkrüger, B., and Giertz, S. (2013). A comparison of hydrological models for assessing the impact of land use and climate change on discharge in a tropical catchment. *J. Hydrol.*, 498, 221–236.

de Marsily, G. (2007). An overview of the world's water resources problems in 2050. *Ecohydrol. Hydrobiol.*, 7, 147–155.

Dembélé, M., Schaefli, B., van de Giesen, N., and Mariéthoz, G. (2020). Suitability of 17 gridded rainfall and temperature datasets for large-scale hydrological modelling in West Africa. *Hydrol. Earth Syst. Sci.*, 24, 5379–5406.

Dembélé, M., Vrac, M., Ceperley, N., Zwart, S. J., Larsen, J., Dadson, S. J., Mariéthoz, G., and Schaefli, B. (2022). Contrasting changes in hydrological processes of the Volta River basin under global warming. *Hydrol. Earth Syst. Sci.*, 26, 1481–1506.

Descroix, L., Guichard, F., Grippa, M., Lambert, L., Panthou, G., Mahé, G., Gal, L., Dardel, C., Quantin, G., Kergoat, L., Bouaïta, Y., Hiernaux, P., Vischel, T., Pellarin, T., Faty, B., Wilcox, C., Malam Abdou, M., Mamadou, I., Vandervaere, J.-P., Diongue-Niang, A., Ndiaye, O., Sané, Y., Dacosta, H., Gosset, M., Cassé, C., Sultan, B., Barry, A., Amogu, O., Nka Nnomo, B., Barry, A., and Paturel, J.-E. (2018). Evolution of surface hydrology in the Sahelo-Sudanian strip: an updated review. *Water*, 10, article no. 748.

Dey, P. and Mishra, A. (2017). Separating the impacts of climate change and human activities on streamflow: A review of methodologies and critical assumptions. *J. Hydrol.*, 548, 278–290.

Diedhiou, A., Bichet, A., Wartenburger, R., Seneviratne, S. I., Rowell, D. P., Sylla, M. B., Diallo, I., Todzo, S., Touré, N. E., Camara, M., Ngatchah, B. N., Kane, N. A., Tall, L., and Affholder, F. (2018). Changes in climate extremes over West and Central Africa at 1.5 °C and 2 °C global warming. *Environ. Res. Lett.*, 13, article no. 065020.

Dieng, D., Cannon, A. J., Laux, P., Hald, C., Adeyeri, O., Rahimi, J., Srivastava, A. K., Mbaye, M. L., and Kunstmann, H. (2022). Multivariate bias-correction of high-resolution regional climate change simulations for West Africa: performance and climate change implications. *JGR Atmos.*, 127(5), article no. e2021JD034836.

Dosio, A., Turner, A. G., Tamoffo Tchio, A., Sylla, M. B., Lennard, C., Jones, R., Terray, L., Nikulin, G., and Hewitson, B. (2020). A tale of two futures: contrasting scenarios of future precipitation for West Africa from an ensemble of regional climate models. *Environ. Res. Lett.*, 15(6), article no. 064007.

Eyring, V., Bony, S., Meehl, G. A., Senior, C. A., Stevens, B., Stouffer, R. J., and Taylor, K. E. (2016). Overview of the coupled model intercomparison project phase 6 (CMIP6) experimental design and organization. *Geosci. Model Dev.*, 9, 1937–1958.

Fovet, O., Belemtougri, A., Boithias, L., Braud, I., Charlier, J., Cottet, M., Daudin, K., Dramais, G., Ducharne, A., Folton, N., Grippa, M., Hector, B., Kuppel, S., Le Coz, J., Legal, L., Martin, P., Moatar, F., Molénat, J., Probst, A., Riotte, J., Vidal, J., Vinatier, F., and Datry, T. (2021). Intermittent rivers and ephemeral streams: Perspectives for critical zone science and research on socio-ecosystems. *WIREs Water*, 8(4), article no. e1523.

Gal, L., Grippa, M., Hiernaux, P., Pons, L., and Kergoat, L. (2017). The paradoxical evolution of runoff

in the pastoral Sahel: analysis of the hydrological changes over the Agoufou watershed (Mali) using the KINEROS-2 model. *Hydrol. Earth Syst. Sci.*, 21, 4591–4613.

Gao, J., Sheshukov, A. Y., Yen, H., Douglas-Mankin, K. R., White, M. J., and Arnold, J. G. (2019). Uncertainty of hydrologic processes caused by bias-corrected CMIP5 climate change projections with alternative historical data sources. *J. Hydrol.*, 568, 551–561.

Gbohoui, Y. P., Paturel, J.-E., Tazen, F., Mounirou, L. A., Yonaba, R., Karambiri, H., and Yacouba, H. (2021). Impacts of climate and environmental changes on water resources: A multi-scale study based on Nakanbé nested watersheds in West African Sahel. *J. Hydrol.: Reg. Stud.*, 35, article no. 100828.

Gbohoui, Y. P., Yonaba, R., Fowé, T., Paturel, J.-E., Karambiri, H., and Yacouba, H. (2022). Comparison of One-Site vs Multi-Sites calibration/validation schemes for hydrological modelling of nested watersheds in the West African Sahel (No. IAHS2022-69). In *Presented at the IAHS2022, Copernicus Meetings, Montpellier, France*.

Grippa, M., Kergoat, L., Boone, A., Peugeot, C., Demarty, J., Cappelaere, B., Gal, L., Hiernaux, P., Mougin, E., Ducharne, A., Dutra, E., Anderson, M., Hain, C., and ALMIP2 working group (2017). Modeling surface runoff and water fluxes over contrasted soils in the pastoral sahel: evaluation of the ALMIP2 land surface models over the Gourma Region in Mali. *J. Hydrometeorol.*, 18, 1847–1866.

Hargreaves, G. H. and Samani, Z. A. (1985). Reference crop evapotranspiration from temperature. *Appl. Eng. Agric.*, 1, 96–99.

Hattermann, F. F., Vetter, T., Breuer, L., Su, B., Daggupati, P., Donnelly, C., Fekete, B., Flörke, F., Gosling, S. N., Hoffmann, P., Liersch, S., Masaki, Y., Motovilov, Y., Müller, C., Samaniego, L., Stacke, T., Wada, Y., Yang, T., and Krysnaova, V. (2018). Sources of uncertainty in hydrological climate impact assessment: a cross-scale study. *Environ. Res. Lett.*, 13, article no. 015006.

Hounkpè, J., Diekkrüger, B., Afouda, A. A., and Sintondji, L. O. C. (2019). Land use change increases flood hazard: a multi-modelling approach to assess change in flood characteristics driven by socio-economic land use change scenarios. *Nat. Hazards*, 98, 1021–1050.

Ibrahim, B. (2002). Analyse de la variabilité climatique au Burkina Faso au cours de la seconde moitié du 20ème siècle - Sécheresse info. http://www.secheresse.info/spip.php?article55865. Master thesis, Institut International d'Ingénierie de l'Eau et de l'Environnement.

Idrissou, M., Diekkrüger, B., Tischbein, B., Op de Hipt, F., Näschen, K., Poméon, T., Yira, Y., and Ibrahim, B. (2022). Modeling the impact of climate and land use/land cover change on water availability in an inland valley catchment in Burkina Faso. *Hydrology*, 9, article no. 12.

IGB (2002). Base de données d'Occupation des Terres (BDOT) 2002. https://www.unoosa.org/documents/pdf/psa/activities/2007/morocco/presentations/4-6.pdf. Burkina Faso.

IPCC (2022). Summary for policymakers. In Pörtner, H. O., Roberts, D. C., Tignor, M., Poloczanska, E. S., Mintenbeck, K., Alegria, A., Craig, M., Langsdorf, S., Löschke, S., Möller, V., Okem, A., and Rama, B., editors, *Climate Change 2022: Impacts, Adaptation, and Vulnerability. Contribution of Working Group II to the Sixth Assessment Report of the Intergovernmental Panel on Climate Change*, pages 3–33. Cambridge University Press, Cambridge, UK and New York, NY, USA.

Kafando, M. B., Koïta, M., Le Coz, M., Yonaba, O. R., Fowe, T., Zouré, C. O., Faye, M. D., and Leye, B. (2021). Use of multidisciplinary approaches for groundwater recharge mechanism characterization in basement aquifers: case of sanon experimental catchment in Burkina Faso. *Water*, 13, article no. 3216.

Karambiri, H., García Galiano, S. G., Giraldo, J. D., Yacouba, H., Ibrahim, B., Barbier, B., and Polcher, J. (2011). Assessing the impact of climate variability and climate change on runoff in West Africa: the case of Senegal and Nakambe River basins. *Atmos. Sci. Lett.*, 12, 109–115.

Karambiri, H., Ribolzi, O., Delhoume, J. P., Ducloux, J., Coudrain-Ribstein, A., and Casenave, A. (2003). Importance of soil surface characteristics on water erosion in a small grazed Sahelian catchment. *Hydrol. Process.*, 17, 1495–1507.

Laux, P., Rötter, R. P., Webber, H., Dieng, D., Rahimi, J., Wei, J., Faye, B., Srivastava, A. K., Bliefernicht, J., Adeyeri, O., Arnault, J., and Kunstmann, H. (2021). To bias correct or not to bias correct? An agricul-

tural impact modelers' perspective on regional climate model data. *Agric. For. Meteorol.*, 304–305, article no. 108406.

Lèye, B., Zouré, C. O., Yonaba, R., and Karambiri, H. (2021). Water resources in the sahel and adaptation of agriculture to climate change: Burkina Faso. In Diop, S., Scheren, P., and Niang, A., editors, *Climate Change and Water Resources in Africa*, pages 309–331. Springer International Publishing, Cham.

Li, Z., Li, Z., Zhao, W., and Wang, Y. (2015). Probability modeling of precipitation extremes over two river Basins in Northwest of China. *Adv. Meteorol.*, 2015, article no. 374127.

Mahé, G. and Paturel, J.-E. (2009). 1896–2006 Sahelian annual rainfall variability and runoff increase of Sahelian Rivers. *C. R. Geosci.*, 341, 538–546.

Maraun, D. (2016). Bias correcting climate change simulations—a critical review. *Curr. Clim. Change Rep.*, 2, 211–220.

Mbaye, M. L., Haensler, A., Hagemann, S., Gaye, A. T., Moseley, C., and Afouda, A. (2016). Impact of statistical bias correction on the projected climate change signals of the regional climate model REMO over the Senegal River Basin. *Int. J. Climatol.*, 36, 2035–2049.

Moriasi, D. N., Pai, N., Steiner, J. L., Gowda, P. H., Winchell, M., Rathjens, H., Starks, P. J., and Verser, J. A. (2019). SWAT-LUT: a desktop graphical user interface for updating Land Use in SWAT. *J. Am. Water Resour. Assoc.*, 55, 1102–1115.

Mounirou, L. A. (2012). *Etude du ruissellement et de l'érosion à différentes échelles spatiales sur le bassin versant de Tougou en zone sahélienne du Burkina Faso: quantification et transposition des données*. PhD thesis, Université des sciences et techniques de Montpellier 2.

Mounirou, L. A., Yonaba, R., Koïta, M., Paturel, J.-E., Mahé, G., Yacouba, H., and Karambiri, H. (2021). Hydrologic similarity: Dimensionless runoff indices across scales in a semi-arid catchment. *J. Arid Environ.*, 193, article no. 104590.

Mounirou, L. A., Zouré, C. O., Yonaba, R., Paturel, J.-E., Mahé, G., Niang, D., Yacouba, H., and Karambiri, H. (2020). Multi-scale analysis of runoff from a statistical perspective in a small Sahelian catchment under semi-arid climate. *Arab. J. Geosci.*, 13, article no. 154.

Ndiaye, P. M., Bodian, A., Diop, L., and Djaman, K. (2017). Évaluation de vingt méthodes d'estimation de l'évapotranspiration journalière de référence au Burkina Faso. *Physio-Géo*, 11, 129–146.

Neitsch, S., Arnold, J., Kiniry, J. R., and Williams, J. R. (2011). *Soil and Water Assessment Tool theoretical documentation: Version 2009*. Texas Water Resources Institute, Texas, USA.

Nyamekye, C., Thiel, M., Schönbrodt-Stitt, S., Zoungrana, B., and Amekudzi, L. (2018). Soil and water conservation in Burkina Faso, West Africa. *Sustainability*, 10, article no. 3182.

Olivera, S. and Heard, C. (2019). Increases in the extreme rainfall events: Using the Weibull distribution. *Environmetrics*, 30, article no. e2532.

Onyutha, C., Turyahabwe, C., and Kaweesa, P. (2021). Impacts of climate variability and changing land use/land cover on River Mpanga flows in Uganda, East Africa. *Environ. Challenges*, 5, article no. 100273.

Pai, N. and Saraswat, D. (2011). SWAT2009_LUC: a tool to activate the land use change module in SWAT 2009. *Trans. ASABE*, 54, 1649–1658.

Panthou, G., Lebel, T., Vischel, T., Quantin, G., Sane, Y., Ba, A., Ndiaye, O., Diongue-Niang, A., and Diopkane, M. (2018). Rainfall intensification in tropical semi-arid regions: the Sahelian case. *Environ. Res. Lett.*, 13, article no. 064013.

Paturel, J. E., Mahé, G., Diello, P., Barbier, B., Dezetter, A., Dieulin, C., Karambiri, H., Yacouba, H., and Maiga, A. (2017). Using land cover changes and demographic data to improve hydrological modeling in the Sahel: Improving hydrological modelling in the Sahel. *Hydrol. Process.*, 31, 811–824.

Popp, A., Calvin, K., Fujimori, S., Havlik, P., Humpenöder, F., Stehfest, E., Bodirsky, B. L., Dietrich, J. P., Doelmann, J. C., Gusti, M., Hasegawa, T., Kyle, P., Obersteiner, M., Tabeau, A., Takahashi, K., Valin, H., Waldhoff, S., Weindl, I., Wise, M., Kriegler, E., Lotze-Campen, H., Fricko, O., Riahi, K., and van Vuuren, D. P. (2017). Land-use futures in the shared socio-economic pathways. *Glob. Environ. Change*, 42, 331–345.

Raziei, T. and Pereira, L. S. (2013). Estimation of ETo with Hargreaves–Samani and FAO-PM temperature methods for a wide range of climates in Iran. *Agric. Water Manage.*, 121, 1–18.

Rusagara, R., Koïta, M., Plagnes, V., and Jost, A. (2022). Groundwater recharge pathways to a weathered-rock aquifer system in a dryland catchment in Burkina Faso. *Hydrogeol. J.*, 30, 1489–1512.

Satgé, F., Defrance, D., Sultan, B., Bonnet, M.-P., Seyler, F., Rouché, N., Pierron, F., and Paturel, J.-E. (2020). Evaluation of 23 gridded precipitation datasets across West Africa. *J. Hydrol.*, 581, article no. 124412.

Sawadogo, B. and Barro, D. (2022). Space-time trend detection and dependence modeling in extreme event approaches by functional peaks-over-thresholds: application to precipitation in Burkina Faso. *Int. J. Math. Math. Sci.*, 2022, article no. 2608270.

Séguis, L., Cappelaere, B., Milési, G., Peugeot, C., Massuel, S., and Favreau, G. (2004). Simulated impacts of climate change and land-clearing on runoff from a small Sahelian catchment: Climatic and anthropogenic effects on Sahelian runoff. *Hydrol. Process.*, 18, 3401–3413.

Serdeczny, O., Adams, S., Baarsch, F., Coumou, D., Robinson, A., Hare, W., Schaeffer, M., Perrette, M., and Reinhardt, J. (2017). Climate change impacts in Sub-Saharan Africa: from physical changes to their social repercussions. *Reg. Environ. Change*, 17, 1585–1600.

Sidibe, M., Dieppois, B., Eden, J., Mahé, G., Paturel, J.-E., Amoussou, E., Anifowose, B., and Lawler, D. (2019). Interannual to Multi-decadal streamflow variability in West and Central Africa: Interactions with catchment properties and large-scale climate variability. *Glob. Planet. Change*, 177, 141–156.

Stanzel, P., Kling, H., and Bauer, H. (2018). Climate change impact on West African rivers under an ensemble of CORDEX climate projections. *Clim. Serv.*, 11, 36–48.

Sylla, M. B., Pal, J. S., Faye, A., Dimobe, K., and Kunstmann, H. (2018). Climate change to severely impact West African basin scale irrigation in 2 °C and 1.5 °C global warming scenarios. *Sci. Rep.*, 8, article no. 14395.

Taylor, C. M., Belušić, D., Guichard, F., Parker, D. J., Vischel, T., Bock, O., Harris, P. P., Janicot, S., Klein, C., and Panthou, G. (2017). Frequency of extreme Sahelian storms tripled since 1982 in satellite observations. *Nature*, 544, 475–478.

Tazen, F., Diarra, A., Kabore, R. F. W., Ibrahim, B., Bologo/Traoré, M., Traoré, K., and Karambiri, H. (2019). Trends in flood events and their relationship to extreme rainfall in an urban area of Sahelian West Africa: The case study of Ouagadougou, Burkina Faso. *J. Flood Risk Manage.*, 12, article no. e12507.

Tazen, F., Paturel, J.-E., and Karambiri, H. (2013). Impacts des changements globaux sur les ressources en eau dans la zone sahélienne en Afrique de l'Ouest. In *IAHS-AISH Publication*, pages 99–104. International Association of Hydrological Sciences, Gothenburg, Sweden.

Todzo, S., Bichet, A., and Diedhiou, A. (2020). Intensification of the hydrological cycle expected in West Africa over the 21st century. *Earth Syst. Dynam.*, 11, 319–328.

Tomer, M. D. and Schilling, K. E. (2009). A simple approach to distinguish land-use and climate-change effects on watershed hydrology. *J. Hydrol.*, 376, 24–33.

Tramblay, Y., Villarini, G., and Zhang, W. (2020). Observed changes in flood hazard in Africa. *Environ. Res. Lett.*, 15, article no. 1040b5.

Valentin, C. (2018). Soil surface crusting of soil and water harvesting. In Valentin, C., editor, *Soils as a Key Component of the Critical Zone 5*, pages 21–38. John Wiley & Sons, Inc., Hoboken, NJ, USA.

Wagner, P. D., Bhallamudi, S. M., Narasimhan, B., Kantakumar, L. N., Sudheer, K. P., Kumar, S., Schneider, K., and Fiener, P. (2016). Dynamic integration of land use changes in a hydrologic assessment of a rapidly developing Indian catchment. *Sci. Total Environ.*, 539, 153–164.

Wallach, D., Mearns, L. O., Ruane, A. C., Rötter, R. P., and Asseng, S. (2016). Lessons from climate modeling on the design and use of ensembles for crop modeling. *Clim. Chang.*, 139, 551–564.

Yang, Q., Wang, Q. J., Hakala, K., and Tang, Y. (2021). Bias-correcting input variables enhances forecasting of reference crop evapotranspiration. *Hydrol. Earth Syst. Sci.*, 25, 4773–4788.

Yin, J., He, F., Xiong, Y. J., and Qiu, G. Y. (2017). Effects of land use/land cover and climate changes on surface runoff in a semi-humid and semi-arid transition zone in northwest China. *Hydrol. Earth Syst. Sci.*, 21, 183–196.

Yira, Y., Diekkrüger, B., Steup, G., and Bossa, A. Y. (2017). Impact of climate change on hydrological conditions in a tropical West African catchment using an ensemble of climate simulations. *Hydrol. Earth Syst. Sci.*, 21, 2143–2161.

Yonaba, R., Belemtougri, A., Tazen, F., Mounirou, L. A., Koïta, M., Karambiri, H., and Yacouba, H. (2022). Assessing the accuracy of SM2RAIN (Soil

Moisture to Rainfall) products in poorly gauged countries: the case of Burkina Faso in the West African Sahel. (No. IAHS2022-263). In *Presented at the IAHS2022, Copernicus Meetings, Montpellier, France*.

Yonaba, R., Biaou, A. C., Koïta, M., Tazen, F., Mounirou, L. A., Zouré, C. O., Queloz, P., Karambiri, H., and Yacouba, H. (2021a). A dynamic land use/land cover input helps in picturing the Sahelian paradox: Assessing variability and attribution of changes in surface runoff in a Sahelian watershed. *Sci. Total Environ.*, 757, article no. 143792.

Yonaba, R., Koïta, M., Mounirou, L. A., Tazen, F., Queloz, P., Biaou, A. C., Niang, D., Zouré, C., Karambiri, H., and Yacouba, H. (2021b). Spatial and transient modelling of land use/land cover (LULC) dynamics in a Sahelian landscape under semi-arid climate in northern Burkina Faso. *Land Use Policy*, 103, article no. 105305.

Yonaba, R. O. (2020). *Dynamique spatio-temporelle des états de surface et influence sur le ruissellement sur un bassin de type sahélien: cas du bassin de Tougou (Nord Burkina Faso)*. PhD thesis, Institut International d'Ingénierie de l'Eau et de l'Environnement.

Zipper, S. C., Motew, M., Booth, E. G., Chen, X., Qiu, J., Kucharik, C. J., Carpenter, S. R., and Loheide II, S. P. (2018). Continuous separation of land use and climate effects on the past and future water balance. *J. Hydrol.*, 565, 106–122.

Zouré, C., Queloz, P., Koïta, M., Niang, D., Fowé, T., Yonaba, R., Consuegra, D., Yacouba, H., and Karambiri, H. (2019). Modelling the water balance on farming practices at plot scale: Case study of Tougou watershed in Northern Burkina Faso. *Catena*, 173, 59–70.

Zouré, C. O. (2019). Étude des performances hydrologiques des techniques culturales dans un contexte de changement climatique en zone sahélienne du Burkina Faso. PhD thesis, Institut International d'Ingénierie de l'Eau et de l'Environnement.